Kent Academic Repository

Manyanya, Nyasha (2018) *Lipid vesicle binding and modulation of membrane binding proteins and compounds.* **Master of Science by Research (MScRes) thesis, University of Kent,.**

Lipid vesicle binding and modulation of membrane binding proteins

By Nyasha Manyanya

Faculty of Sciences

School of Biosciences

Master's Research Thesis

Supervisor: Dan Mulvihill

_____

Abstract

<u>Lipid vesicle binding and modulation of membrane binding proteins and compounds.</u>

The lipid bilayer is an essential component of cells that separates the internal components to the external environment and also defines the internal components. Various proteins are utilized by the membrane for various cell processes including signaling, communication and responding to external signals. The interaction between cell membranes and proteins may have biological consequences [Lemmon MA, 2008[1]], so studying these interactions allows a deeper understanding of biological processes and may reveal the pathogenesis of diseases related to these proteins.

Class 1 Myosins are a group of actin based motor proteins associated with various roles related to membrane dynamics and trafficking. Their tail domain contains membrane binding regions such as the TH1 domain and a pleckstrin homology (PH) domain within the TH1.

Alpha Synuclein is a predominantly presynaptic neuronal protein linked to several neurodegenerative disorders such as Parkinson's disease. It has been shown to interact with membranes and to associate with synaptic vesicles. In its physiological state, it has been shown to be acetylated, however the effect of this modification is still being investigated.

Bacterial resistance to antimicrobials is becoming a significant challenge in effective treatment and prevention of bacterial infections worldwide, and the need for new antimicrobials is rising. For antimicrobials to be successful, they must initially penetrate and interact with the bacterial membranes in order to carry out their function.

This project focused on the membrane binding effects of Myosin 1 and alpha Synuclein in order to determine their function and whether post-translational modifications impact these interactions. We also looked at antibiotic compounds to determine their membrane interactions using lipid vesicles as a model for the cell membrane and analyzing the interaction using stopped flow, DLS (dynamic light scattering) data and microscopy images. We successfully cloned and expressed both forms of the TH1 domain and were able to analyze the interaction between alpha Synuclein and vesicles. Our results suggest that the lipid composition of the vesicles affects their interaction with alpha Synuclein. Furthermore, acetylation of alpha Synuclein alters these interactions.

---

[1] Lemmon MA. (2008) *Membrane recognition by phospholipid-binding domains*. Nature Reviews Molecular Cell Biology; **9**: 99-111

Contents

Acknowledgements

I would like to thank my supervisors Dr. Dan Mulvihill and Dr. Jennifer Hiscock and all the members of the Mulvihill-Geeves lab and the Hiscock lab. I would also like to thank my fiancé Max Allen and my family for all their support.

Additional Information

Thesis Information

Word Count: 14884

Page Count: 65

Font: Arial

Size: 12

Abbreviations

αS / αSynuclein– Alpha Synuclein

WT – Wild Type

DM - D mutant

RPM - Revolutions per minute

OD - Optical Density

CaM - Calmodulin

Chapter 1

Introduction

1.1 - The Phospholipid Bilayer
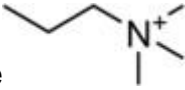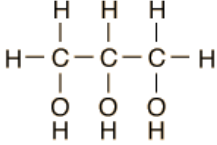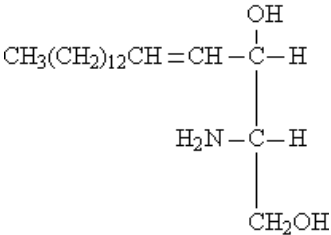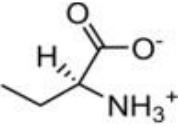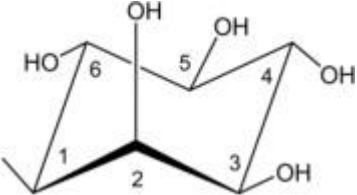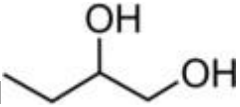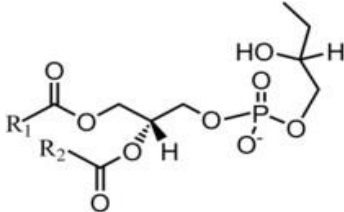
Cell membranes are essential for the structure and function of cells and organelles. They define internal components of cells, separate the internal and external environments and utilize various proteins for communication, signal response and mediating transport [1]. The fundamental building blocks of these membranes are amphipathic phospholipids [2] that are made up of a backbone (*Figure 1)*, which can be either glycerol (named Glycerophospholipids or Phosphoglycerides) or sphingosine (named Sphingomyelins), a polar phosphate head group and apolar fatty acyl chains [3].
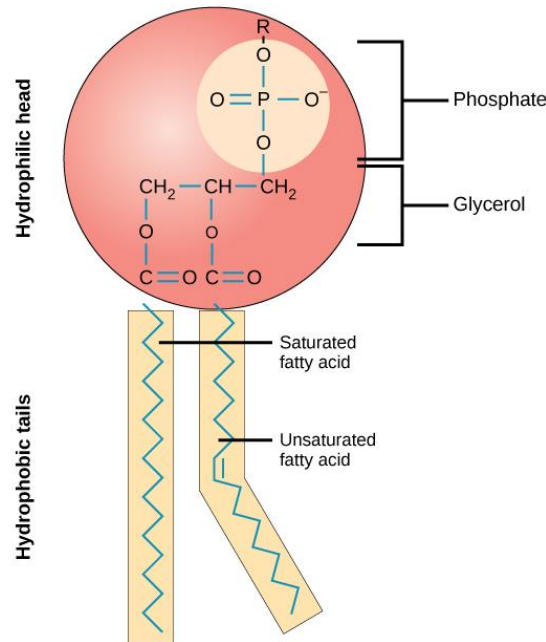
Figure 1: **The structure of a Glycerophospholipid.** Glycerophospholipids are made up of a phosphate head group, fatty acids that can either be saturated or unsaturated and a glycerol molecule joining the hydrophobic and hydrophilic portions together. [2]

Variations in the head groups and fatty acyl chains give rise to different phospholipids *(Table 1)* which allows them to have a large range of functions and to localize in a specific places [4]. The polymorphic capabilities of phospholipids allow them to form bilayers in physiological conditions, which are formed by the hydrophilic head group interacting with the aqueous environment and the hydrophobic tails repelling the aqueous environment and interacting with each other (*Figure 2*). This structure controls transportation across the membrane, provides fluidity, shape and stability to the membrane and allows proteins to be embedded within the membrane without adversely affecting the integrity of the membrane.

Table 1: Phospholipid head group and backbone variations. Different head groups, acyl chains and phospholipid backbones result in a variety of properties, functions and localization [2-6].

Head Group	Backbone
Phosphatidic Acid ⌐H	Glycerophospholipids
Phosphatidylcholine	
Phosphatidylethanolamine	Sphingomyelins
Phosphatidylserine	
Phosphatidylinositol	
PhosphatidylGlycerol	
CardioLipin	
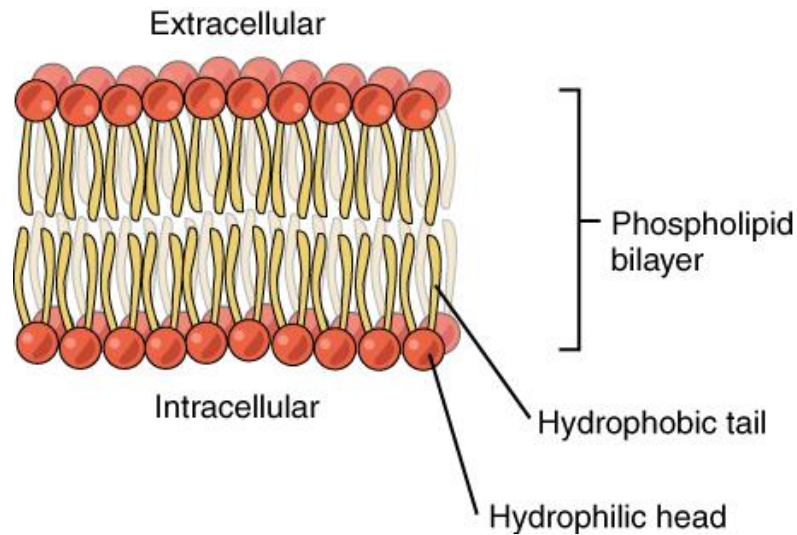
Figure 2: Self-assembly of phospholipids in a membrane. The bilayer is formed when the hydrophilic heads (red) interact with the external aqueous environment, whilst the hydrophobic tails (yellow) are repelled by the aqueous environment and interact with each other [2].

1.2 –Proteins and Binding sites

Proteins are macromolecules that carry out many of the vital functions of cells. During protein folding, the specific amino acids that make up proteins gather together forming 3-D structures that create the protein binding sites. The amino acids that aren't part of the binding site provide a backbone or a support that allows the binding sites to fold into specific shapes, and so changing the amino acid sequence can change the structure and may therefore impact the binding site [6].
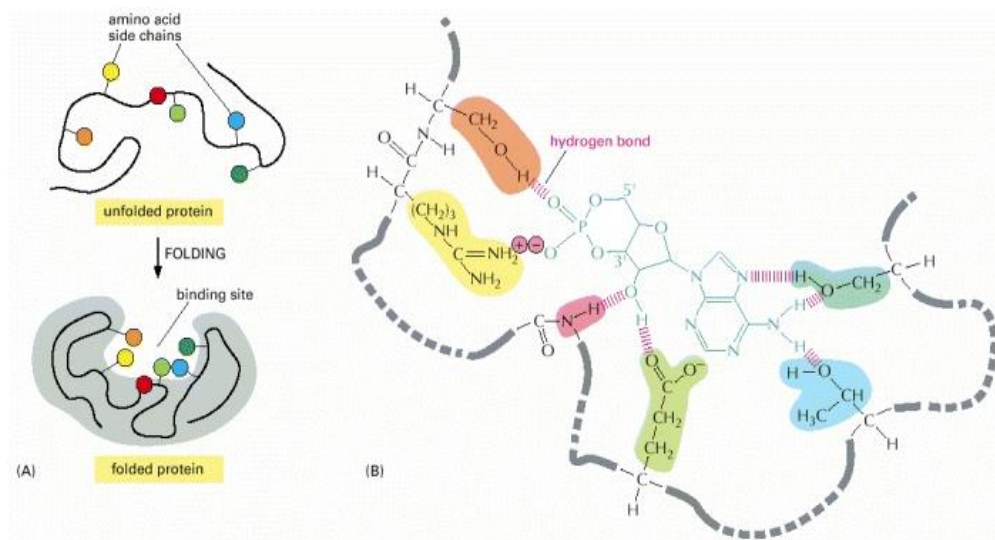
Figure 3: Diagram depicting Protein folding to form a binding site; specific amino acids gather together to form binding sites, and are held together by hydrogen bonds, the surrounding amino acids provide a backbone or support for the binding site [7]

All proteins bind to other molecules through the highly specific binding sites and the molecules a protein interacts with determines its properties. Binding to these molecules is dependent on the ability to form multiple weak non-covalent bonds with other molecules, again allowing for high specificity as the binding molecule (ligand) would need to closely fit the binding site in order to form these bonds. Proteins often contain several binding site so that they can be regulated and for localization, for example, the SH2 protein domain allows proteins to localize in plasma membranes in response to specific signals [7].

1.2.1 – Membrane Proteins
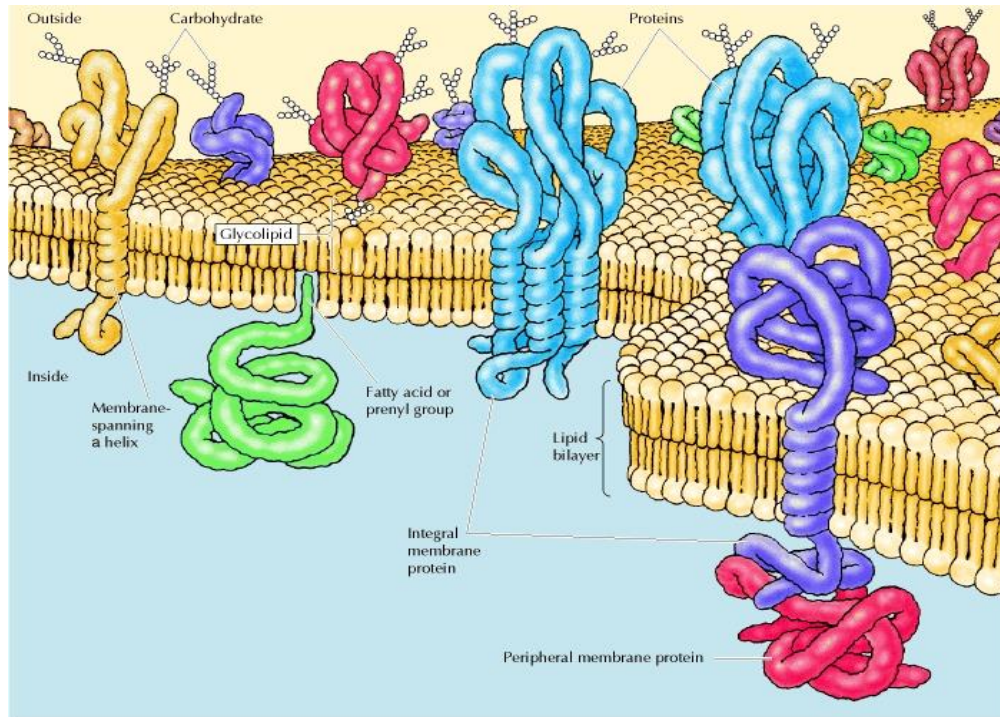
Figure 4: Model of a typical membrane with associated proteins. A variety of amphipathic proteins can associate with the bilayer. They can be intrinsic proteins; whereby the protein is embedded within the bilayer with part of the protein exposed to the environment on one side or both sides of the bilayer (shown here are the blue, purple and yellow proteins). Or they can be external proteins that are bound to the membrane through the use of other intrinsic proteins or hydrophobic groups, which are the peripheral proteins (shown here by the pink and green proteins) [1].

Membrane associated proteins carry out the specific functions for membranes, including external signal response, transportation and mediating interactions between cells [8]. Like the phospholipids, they tend to be amphipathic; their hydrophobic regions interacting with the fatty acyl chains and hydrophilic regions interacting with the head regions. Membrane proteins are divided into two general classes; integral proteins and peripheral proteins which either interact with the membrane integral proteins or with the hydrophilic head groups [9].

Integral or intrinsic membrane proteins are proteins that are embedded directly within the bilayer that can either span across the membrane (making them transmembrane

proteins) or are embedded on one side of the membrane [1]. Due to their ability to span across both hydrophilic and hydrophobic parts of the membrane, they tend to be amphiphilic. The fluidity of the membrane as well as their amphiphilic nature allows them to move freely within membranes and perform functions inside and outside of the cell. Integral proteins are involved in a variety of membrane related functions including cell adhesion, transportation and can act as receptors, enzymes and anchoring domains [8].

Peripheral, or extrinsic membrane proteins are attached to the exterior of the membrane or associate with temporarily and without damage to the membrane. These proteins typically function as regulatory proteins, regulating processes such as cell signaling, enzymatic reactions and activation of membrane activity [1]. Due to their hydrophilic nature, they associate with membranes through intrinsic proteins embedded within the membrane or through electrostatic interactions with the negatively charged head groups, but do not interact with the hydrophobic core of the bilayer [8, 9].

Outside of the protein-phospholipid bilayer is a coat, termed the "Glycocalyx"; an external coat made up of carbohydrate chains that has a variety of functions including providing protection for the cell from damage, retaining moisture and in some cases mediating the cell's interactions [10, 11].

1.2.2 – Post translational modifications

Protein regulation is essential, as it allows proteins to be rapidly adaptable to their environments and allows cells to specialize. Post-translational modifications are protein modifications that occur after translation, whereby functional groups are covalently added to the protein. These include phosphorylation, acetylation and ubiquitination, and are often used in protein regulation within cells [12].

Phosphorylation is the reversible addition of a phosphate group to an amino acid chain of a protein. This happens when the terminal phosphate group on ATP is attached to a hydroxyl group (catalyzed by Protein Phosphatase) forming ADP and the phosphorylated protein [12]. Each phosphate group carries a 2+ charge, which changes the overall charge of the protein and can either change the molecules the protein binds to or change a binding site on allosterically, which can then affect the activity, structure and localization of the protein. Both phosphorylation and de-phosphorylation can be used to turn proteins on or off, allowing the protein to be regulated [1] (Figure 3).
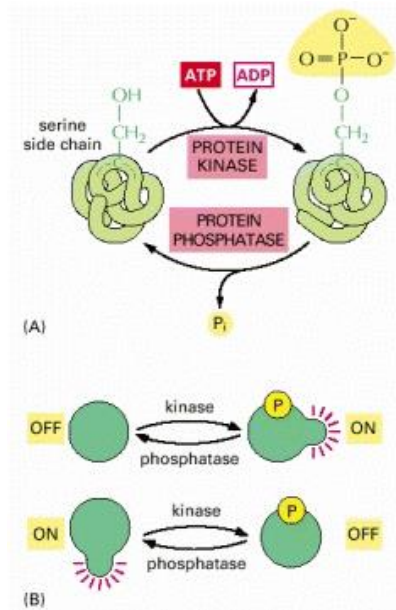
Figure 5: Diagram depicting protein phosphorylation; phosphorylation of proteins is catalyzed by protein kinases with the release of ADP, and de-phosphorylation is catalyzed by phosphatases. Both processes can be used to switch cell processes "on" or "off". [6]

Another post-translational modification used by cells is acetylation. This is the addition of an acetyl group from acetyl co-enzyme A to a protein. Similar to phosphorylation, this allows the cell to respond to specific signals and adapt to its environment quickly [12]. Acetylation occurs in two forms: N-terminal acetylation, which is catalyzed by N-terminal acetyltransferases (NATS) and ϵ-amino group acetylation of lysine (which is less common) [13].

Defects in posttranslational modifications have been linked to diseases, which has led to further research into the effect of these modifications on different proteins. The TH1 domain of Myosin 1 and Alpha synuclein (αSynuclein) are discussed in this study.

1.3 – Myosin

The myosin superfamily are a group of ATP dependent motor proteins that are involved in motility functions [14], most commonly known for muscle contractions. The majority of Myosins localize in the cytoplasm, however some have been found to localize in the nucleus as well, carrying out a range of functions [15]. Some are ubiquitous whilst others are specialized in specific cells, such as mediating cell division, enabling neuronal structural changes and muscle movement and contraction. Although there are many types of myosin with differing functions, they all share the same basic properties; all bind to the cytoskeletal protein actin, converting energy from ATP hydrolysis into mechanical movement to carry out various functions [16-18]. Actin is an abundant protein in eukaryotic cells, with the ability to form microfilaments and thin filaments. Microfilaments are part of the cytoskeleton whereas thin filaments are found in muscle cells and involved in muscle contractions.

1.3.1 – The Myosin Binding Cycle

Myosins walk along these actin filaments in the cytoskeleton and muscle cells, generating mechanical force and allowing movement. Most of the internal and external movements of the body are dependent on this interaction between Myosins and the actin. This interaction involves Myosin molecules undergoing conformational changes, coupled with an increase in the hydrolysis of ATP that enables them to "walk" or slide along actin filaments towards the positively charged end using the "Power stroke" mechanism [19] which is regulated by calcium ion concentration. A complete round of ATP hydrolysis produces a single step or movement along the actin filament. Myosins differ in the way they move along the actin filaments, with some found to even move towards the negatively charged end of actin, however all follow the same basic cycle. Alongside this, Myosins may pull on membranes to change their shape, cause muscle contractions, form tubules along filaments or transport vesicles, lipids and associated proteins along actin molecules [19].
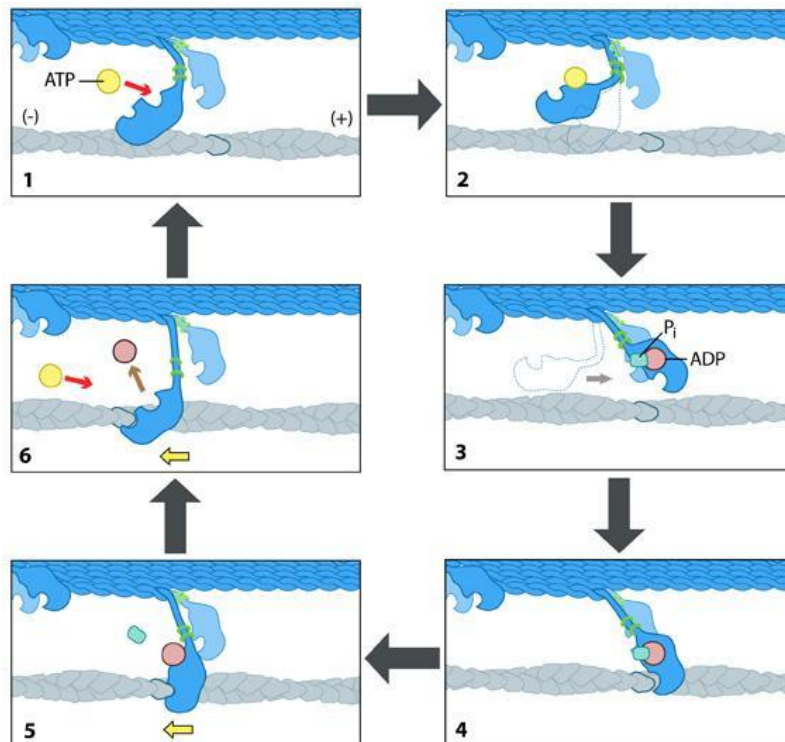
Figure 6: Diagram depicting the "Power stroke" mechanism of Myosins along actin filaments. 1. Unbound myosin is attached to actin, resulting in a conformational change in the myosin molecule. ATP then binds to myosin head domain, inducing a small conformational shift in the actin binding site, leading to myosin releasing the actin filament. **2.** ATP binding also causes the neck region of myosin to bend and position itself further along the filament. **3.** ATP is then hydrolyzed, creating ADP and an inorganic phosphate that are still bound to myosin. **4.** Myosin weakly interacts with actin, causing a conformational change in the myosin head. **5.** Myosin releases Pi, then binds to Actin once again, triggering the power stroke; the force generating step. **6.** Myosin then reverts back to its original conformation and releases ADP. Myosin remains tightly bound to the actin filament at a new position, beginning the cycle once again. **[19]**

1.3.2 – Myosin Domains and Subdomains

All Myosins are made up of 3 separate domains with specific functions; a globular head domain (the N terminal), a neck region and a C-terminal tail region [20].

The motor domain (N-terminal) or the head group, is a generally conserved [20] actin and ATP binding domain made up of 4 subdomains. Isoforms arise from differences in their ability to produce a force against an external load, their regulation and consecutive steps of movement. Some Myosins have single heavy chains, contacting the actin filaments at one site only, while others have two heavy chains which contact Actin on multiple sites [20]. High processive motors (generally polymeric myosin heads) are generally involved in the transportation of cargo whereas low duty motors (monomeric motors) are better suited to rapid movements and contractions of actin [15].
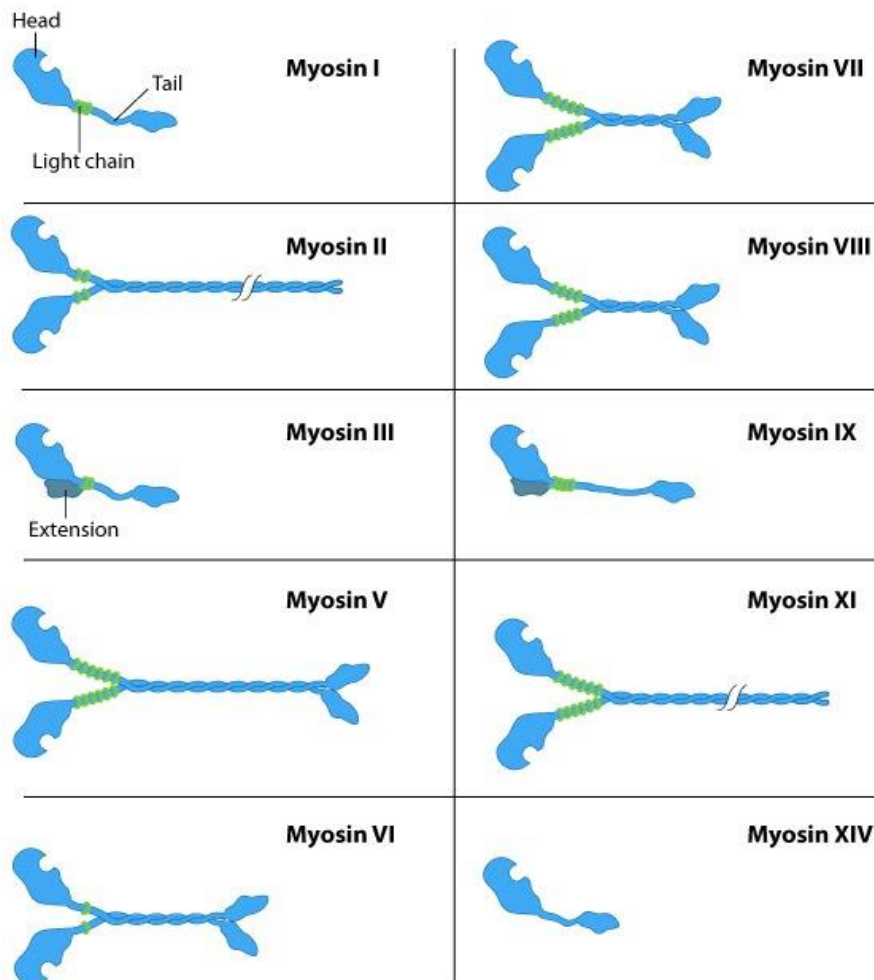
Figure 7: Diagram depicting Myosin Head domain variation. All Myosins have a conserved head domain, where the actin binding site is located, and can vary in the number of heavy chains and thus the number actin binding sites. [15]

Attached to the head domain, it the neck region [21], an alpha helical domain that links the head and the tail domain and regulates Myosin through the use of calmodulin or calmodulin-like light chains [22, 23]. The neck domain acts as a lever arm for the motor domain during the power stroke mechanism, as step size of myosin is linearly related to the length of the neck region [21]. The number and size of light chains attached influence the length of the neck region and therefore the step size of the myosin molecules [20]; the longer the neck domain, the larger the step size. This allows different Myosins to have different functions; larger step sizes being more suitable for sustained binding or transportation of cargo and shorter step sizes being ideal for rapid movements or contractions [21, 24]. Light chains also vary in their mechanism and responses, however all use Ca2+ ion concentration for regulation. An example of these is Calmodulin (CaM), a protein that binds to up to 4 calcium ions (Ca^{2+}), causing conformational changes in CaM, which can either inhibit or activate Myosin, allowing it to be regulated [25-27].

Finally, attached to the neck region is the C-terminal tail domain; the most diverse domain in Myosins. Within the tail domain are regions that determine the function and target of Myosins [18], such as the motor and tail homology 1 domain (TH1) [28]. These subdomains allow them to interact with specific phospholipids and carry out various functions on the cell surface.

The TH1 region contains positively charged regions that electrostatically interact directly with negatively charged phospholipids on cellular membranes which allows them to localize in specific areas. For many molecules, the TH1 domain is essential in localization and function [28]. The TH1 domain contains many regions such as the Pleckstrin Homology domain (PH domain), two membrane-binding regions known as N and C terminal targeting motifs that have been shown to mediate Myosin specificity and binding [29], thereby allowing the TH1 region to regulate the dynamics of Myosin [29]. Other regions include the TH2 region, which has been shown to be a non-ATP sensitive secondary actin binding site, and the TH3 (or SH3) domain [30], which has been shown to organize the actin cytoskeleton, is associated with signal induction and mediate protein-protein interactions by binding to proline-rich structures [31]. The myosin tail can be subdivided into long tailed isoforms and short tailed isoforms that contain the TH1 domain only [28].

The pleckstrin homology domain (PH domain), has drawn research interest due to its ability to interact with Phosphatidylinositol lipids in membranes and proteins [29]. For the most part, this domain interacts in a phospholipid specific manner that may give an indication into the function of certain myosin molecules [29]. PH domains with high affinity have proven to be useful tools in studying biological membranes; when attached to GFP, they allow us to analyze specific phospholipid distribution in cellular membranes. The PH domain is usually implicated in intracellular signaling, the

recruitment of proteins to specific membranes allowing them to localize and carry out specific functions there, or as a part of the cytoskeleton [29].

The PH domain is made up of two perpendicular antiparallel β sheets that differ in length for different isoforms of the PH domain, followed by a c-terminal amphipathic helix that contains a single highly conserved tryptophan. The function of many PH domains, although highly studied, is still unclear [29].

The tail domain provides another mechanism for some Myosins to be regulated called "tail inhibited regulation" [32]. In this model, Myosin tails have 2 conformations; open and folded. When folded, the tail domain interacts with the head domain thereby inhibiting its activity. However when cargo binds or in high Ca^{2+} concentrations, the Myosin becomes open and reduces its interaction with the head domain [33].

Myosins can be divided into two subcategories; conventional and unconventional myosin, determined by their ability to form filaments [16, 28]. Myosin II, one of the most abundant and most commonly known Myosins, is a conventional myosin. Myosin II is involved in muscle contraction and also in driving and mediating motile events in cells. Unconventional Myosins generally have globular head domains and are involved in processes such as endocytosis, intracellular transport, and formation of cell protrusions and gating of ion channels. A common unconventional myosin, and the focus of this study, is Myosin 1.

1.3.3 – Myosin 1

Myosin I (Myo1) proteins are a widely expressed, diverse group of a small monomeric proteins, involved in membrane related processes [28]. They have been shown to associate with cellular organelles such as the Golgi, and dynamic membrane events; endocytosis, exocytosis, membrane trafficking, sensory transduction, cell shape control, cell adhesion [28, 34]. Myosin 1 have also been shown to interact with electrostatically with specific phospholipids [17], however their exact mechanism of action is still unclear, as is their regulation. As they are slow, low duty motor, they are not suited for long range movement or binding, so they exploit diffusion for proper localization and are used in transportation. Isoforms of Myosin 1 have been shown to have differing functions, for example Myo1a has been implicated in the secretion of lysosomal enzymes [34], whereas Myo1c has been shown to be essential in hearing [35], and other myosin isoforms are involved in the transportation of vesicles [36]. Myosin 1 is also found in intestinal brush border cells, where it is involved in membrane-cytoskeletal adhesion to stabilize microvilli [28].

Myosin 1, like other Myosins, can be regulated not only by a calmodulin related light chain, but also by N-terminal phosphorylation, which has attracted much research interest as the both the exact mechanism and the effect that this phosphorylation has on binding are not fully known.

1.4 – Alpha Synuclein

Parkinson's disease (PD) is a progressive neurological condition caused by a loss of nerve cell function and dopamine, a neurotransmitter that regulates movement in the body, the *Substantia Nigra.* PD is more commonly known by symptoms such as rigidity, stiffness and tremors, however its pathogenesis is still unclear. Alpha Synuclein (α-Synuclein), a presynaptic neuronal protein, has been linked to the pathogenesis of PD due to its high prevalence in Lewy bodies (abnormal protein deposits) and its ability to form aggregates [37, 38]. It is abundantly expressed in the nervous system, found close to synaptic vesicles, however, has also been found in erythrocytes and platelets, for unknown reasons [39].

α-Synuclein is coded for by the SNCA gene [37], and several mutations of this gene have been linked to some cases of PD as they cause incorrect folding or an overproduction of αSynuclein [37]. The misfolded or excess αSynuclein is thought to cluster and form aggregates, impairing neuronal function, which is then thought to lead to PD. αSynuclein may also cause dopamine to accumulate at presynaptic terminals, leading to a loss of communication between neurons therefore causing involuntary movement of muscles [40].

The precise role of αSynuclein in the development of PD remains unclear, as is its physiological function [37], however studies suggest it may play a role in maintaining vesicles at presynaptic terminals by aggregating them together, or in the regulation of neurotransmitter release [37, 41]. Although it is natively unstructured in the cytosol, when interacting with membranes αS forms an alpha helical structure that can lead to the formation of oligomers [42].

Three distinct regions make up αS; an amino terminal with lipid binding motif, a central hydrophobic domain called the NAC region, which distinguishes it from the other members of the Synuclein family, and an acidic C-terminus or "tail" region [43]. The N-terminal domain is positively charged and it thought to interact with anionic phospholipids reversibly.

The stability and folding of αS and its membrane related functions, are subject to a variety of post translational modification such as N-terminal acetylation and ubiquitination [43]. N-terminal acetylation of αSynuclein has recently drawn research attention. In its native state, αSynuclein has been found to be N-terminally acetylated and this is thought to regulate its activity. Several models for αSynuclein pathogenesis have surfaced [44-46] and multiple mutations have been linked to PD [47].

Several neurodegenerative diseases, such as PD, Alzheimer's disease and Huntington's disease, have been shown to have similar pathologies; misfolded proteins accumulating to form aggregates leading to neurological degeneration. As this suggests a similar pathogenic mechanism [48-50], understanding the physiological function of αSynuclein may give insight into involvement in PD pathogenesis, thus

allowing us to better understand these other diseases. This could also lead to more effective treatments for these diseases or potentially a cure for these diseases.

1.5 – Aim of this study

The interaction between cell membranes and proteins, in particular peripheral proteins, may have an effect on the membrane dynamics and morphology, and therefore has biological consequences [Lemmon MA, 2008]. The study of these interactions allows a deeper understanding of biological processes and also allows us to determine the pathogenesis of diseases related to these proteins. The aim of this project was to determine how various membrane binding proteins interact with specific phospholipids and how the post-translational modifications acetylation and phosphorylation impact their interactions. Therefore, in this study, we will be looking at how the acetylation of αSynuclein, and similarly how phosphorylation of the TH1 domain of Myosin 1, impact their membrane interactions.

Chapter 2

Materials and Methods

2.1 - Materials

2.1.1 – Bacterial Strains

Escherichia coli: DH10B, BL21 (DE3) PlysS and BL21 (DE3) Cam1 Rosetta competent were used in transformations for plasmid DNA isolation and protein induction.

2.1.2 – Buffers and Media

Luria-Bertani (LB) Media

1 liter of LB was made using 5 g Yeast extract, 10 g Tryptone and 10 g Sodium Chloride added to 1 Liter of dH_2O [51]. This was then stirred using magnetic stirrer until dissolved and then poured into desired bottles or flasks to be autoclaved.

Vesicle Buffer A

Made up of 0.005M NaH_2PO_4 and 0.5M NaCl in dH_2O and pH adjusted to pH 7.2

Native Lysis Buffer B

Made up of 5mM $MgCl_2$, 50mM NaH_2PO_4, 300mM NaCl and 10mM Imidazole in dH_2O and pH adjusted to pH 8.0

Native Wash Buffer B

Made up of 50mM NaH_2PO_4, 300mM NaCl and 20mM Imidazole in dH_2O and pH adjusted to pH 8.0

Native Elution Buffer B

Made up of 50mM NaH_2PO_4, 300mM NaCl and 500mM Imidazole in dH_2O and pH adjusted to pH 8.0

Native Binding buffer A

Made up of 50mM Tris Base, 500mM NaCl and 10mM Imidazole in dH_2O and pH adjusted to pH 7.8

Native Wash Buffer A

Made up of 50mM Tris Base, 500mM NaCl and 10mM Imidazole in dH_2O and pH adjusted to pH 6.0

Native Elution Buffer A

Made up of 50mM Tris Base, 500mM NaCl and 150mM Imidazole in dH_2O and pH adjusted to pH 6.0

Column Wash

Made up of 20mM MES, 30mM NaCl in dH_2O and pH adjusted to pH 5.0

Denaturing Buffer B

Made up of 7M Urea, 0.1M NaH2PO4 and 0.01M Tris base in dH2O and pH adjusted to pH 8.0

Denaturing Buffer C

Made up of 8M Urea, 0.1M NaH2PO4 and 0.01M Tris base in dH2O and pH adjusted to pH 6.3

Denaturing Buffer E

Made up of 8M Urea, 0.1M NaH2PO4 and 0.01M Tris base in dH2O and pH adjusted to pH 4.5

SDS Page Buffer

TAE Buffer

2.1.3 - Gene constructs

The Hum-1 TH1 and Hum-1 C-terminal genes from C-*elegans* were used to create the following constructs using the pTOPO2.1 vector (Invitrogen).

v833 - pET151DTOPO_Nde1hum1TH1 (717-912) BamH1 (WT TH1)

v839 - pET151DTOPO_Nde1hum1 (717) TH1-End BamH1 (WT C-terminal)

v884 - pET151DTOPO_NcoImNeongreen-Nde1hum1TH1 (717-912) BamH1 (Neon green WT TH1)

Phosphomimetic mutants

V875-6 - pET151DTOPO_Nde1hum1TH1S782A (717-912) BamH1

v877 - pET151DTOPO_Nde1hum1TH1S782D (717-912) BamH1

v886 - pET151DTOPO_NcoImNeongreen-Nde1hum1TH1 (717-912) S734D BamH1 (Neon Green D

Each construct was checked once generated using a restriction enzyme digest and then run on an Ethidium Bromide gel, if successful, then sequenced.

The αSynuclein construct **v696** - pETDuet-1_aS-Cerulean3 was created by another member of the lab. The isoforms of αS were generated by transforming the construct into different competent cells. For acetylated αS, *E. coli* BL21 NatB cells were used, whereas the un-acetylated αS was formed using BL21 DE3 pLysS cells.

2.1.4 – DNA and Protein Ladders (Molecular Markers)
- PageRuler™ Unstained Protein Ladder
- New England BioLabs (NEB) 1 kb DNA ladder

2.2 - Methods

2.2.1 – Cell Cultures

E. coli cultures

E. coli cultures were made up using 5ml of Luria-Bertani Media and grown to an optical density at 595nm of 0.4.

2.2.2 – Cloning

Transformations

An aliquot of competent cells were defrosted on ice. 3 µL of desired plasmid was added and mixed gently using a pipette tip. Cells were incubated on ice for 30 minutes before subjecting them to a 90 second heat shock at 42°C then returned to ice for 2 minutes. 100 µL LB was added and then incubated at 37°C while shaking for 1 hour. Cells were plated onto LB agar plate with 5 µL of antibiotic, then incubated overnight at 25°C.

Cloning and expressing the TH1 and Full length tail

The Hum 1 gene from *Caenorhabditis elegans* (C. *elegans*) was used to clone the TH1 domain and the full length tail.

Three sets of oligonucleotides (602, 603 and 604) were created from the Hum 1 gene sequence and ordered from IDT. The oligonucleotides were then diluted to a final concentration of 1µg/µL and mixed as follows:

TH1 Domain: *1ul of oligo 602 was added to 1ul of oligo 604 with 8ul of dH2O*

Full length tail*: 1ul 602 was added to 1ul of oligo 603 with 8ul of dH2O*

High infidelity PCR was conducted on these and then both the TH1 domain and full length tail plasmids were transformed into *E. coli* BL21 DE3 pLysS cells to express this protein for further experiments.

Neon Green TH1

Ligation A

6µL dH20, 1µL T4 Ligase Buffer, 1µL TH1 PCR product, 1µL Pgem Vector and 1µL of DNA Ligase

Ligation B

2µL dH2O, 1µL T4 Ligase Buffer, 5µL PCR product, 1µL Pgem Vector and 1µL of DNA Ligase

Ligations were set up as stated above and incubated at 16 °C overnight then heat inactivated at 65 °C for 10 minutes the following day. A transformation was carried out as normal using DH10B cells, and transformants were plated on LB plates with 5µL Ampicillin, IPTG and Xgal.

2.2.3 – DNA Protocols

DNA Extraction and Purification

Qiagen's QIAquick gel extraction kit and miniprep kit were used according to their instructions [52].

Agarose gel electrophoresis (Ethidium Bromide)

Agarose powder was weighed into an Erlenmeyer flask and dissolving into the appropriate volume of TAE Buffer to make a 0.5% Agarose gel. The agarose-buffer mixture was melted, swirling to mix at regular intervals, and allowed to cool slightly. Ethidium Bromide was added to a final concentration of 0.5 µg/ml and the molten gel was poured into a gel casting tray. Any air bubbles were removed using a pipette tip, then a gel comb was carefully placed along the top of the gel to create wells. The gel was allowed to set at room temperature, then comb was carefully removed and the gel was placed in the gel tank with TAE buffer. Gels were run either 50V for 60 minutes or 100V for 30 minutes then visualized under a UV lamp and imaged.

PCR

PCR was carried out under the following conditions and then run on an Ethidium Bromide gel to determine whether product was present:

Hot start

92℃ for 30 seconds

45℃ 30 seconds

72℃ 1 minute

Repeat steps **2-4** 25 times

2.2.4 – Protein Protocols

Protein Induction

Overnight cultures were set up and used the following day.

Small scale induction

20 ml of LB was poured into a 50 ml Falcon tube with 20µL of each antibiotic needed. 200µL of the overnight culture was added and the falcon tube was incubated at 37°C with shaking. When the culture had reached an optical density of 0.4 abs at 595 nm, a 1 ml sample was taken and kept for SDS PAGE analysis, then 20µL of IPTG was added to the culture and incubated at 37°C with shaking for 2-4 hours.

After induction, cells were harvested by centrifugation at 4600 rpm for 30 minutes at 4°C. Pellets were stored at - 20°C until required.

Large Scale Induction

1 Liter of LB was divided into two 2 Liter conical flasks, a sponge stopper and tin foil were placed in the top of the flasks. The LB was autoclaved for 20 minutes and once cool, 500 µL of each antibiotic required were added to each flask along with 5 ml of the overnight culture. The cultures in the flasks were then incubated at 37°C with shaking until they had reached an optical density of 0.4 at 595 nm, a 1 ml sample was taken and kept for SDS PAGE analysis and 500µL IPTG was added to each flask. The cultures were incubated for another 2-4 hours at 37°C with shaking, then cells were harvested by centrifugation at 8000 rpm for 20 minutes at 4°C. Pellets were stored at -20°C until required.

SDS PAGE Analysis

1 ml samples were extracted every hour after IPTG was added, their optical density was recorded and then the samples were centrifuged in Eppendorfs and pellets were used for SDS PAGE analysis. The optical density of the samples was multiplied by 100 to give the volume of PBS needed to re-suspend them in µL. ¼ of that volume of protein loading buffer was added to the solutions and the protein was denatured by heating at 95°C. 20µL of each sample was run on an SDS PAGE gel.

Protein Purification

Preparation under Native Conditions

Protein pellets were thawed and re-suspended at 2-5 ml per gram weight of either the Native Binding Buffer A or Native Lysis Buffer B. Lysozyme was added to a final concentration of 1mg/ml and incubated for 30 minutes on ice. The solution was then sonicated in six 30 second bursts with 1 minute intervals, then poured into a centrifuge tube and centrifuged at 4600 rpm for 20 minutes at 4℃. The supernatant was collected and 1µL DNase and 1µL RNase were added then incubated on ice for 15 minutes. Protein was isolated by centrifugation at 10000 rpm for 20-30 minutes at 4°C. The supernatant and pellet were carefully separated and the supernatant was kept for purification. 20 µL of each were run on an SDS PAGE gel to check solubility.

Purification under Native conditions using a Cobalt Column

Native Binding Buffer A was used to re-suspend frozen protein pellet.

Tweezers were sterilized using Ethanol and a Bunsen flame and a small amount of sterile cotton was taken out using the sterilized tweezers and pushed into the bottom of a sterile 10 ml needleless syringe. Distilled water was pipetted into the syringe and then pushed down used the plunger, creating a stopper that would prevent the resin from escaping through the syringe. The syringe was then clamped onto a clamp stand and a small cap was placed on the lip of the syringe. 2 ml of Metal Affinity Cobalt Resin was slowly pipetted into the column and allowed to settle, then the cap was removed and the storage fluid was allowed to slowly drip out. 6 ml of water was used to settle

the resin and wash out the storage fluid. 10 ml of Native binding buffer A was slowly and gently pipetted into the syringe, and allowed to drip through, so as to calibrate the column, ensuring the gel doesn't dry out. The cap was replaced on the lip of the syringe and 2 ml of Native Binding Buffer A was added to the top of the gel.

Once sample was prepared, it was loaded slowly into the column, without disturbing the resin. The cap was again removed and the sample was allowed to drip through the resin and caught in bijou tubes. The His-Tagged protein should have bound to the cobalt resin at this point. Native wash buffer A was then pipetted slowly 1 ml at a time, up to a total volume of 10 ml, to wash out unbound protein which was caught in bijou tubes. Once all the wash buffer had run through, the cap was placed on the lip of the syringe to stop the gel from drying out. 10 ml of Native elution buffer A was pipetted gently into the column. The cap was removed and ten 1 ml elutions were collected and all bijou tubes were clearly labelled. 20µL from each sample was taken and saved in an Eppendorf to run on an SDS-PAGE gel. The column was then washed through with Native binding Buffer A and the cap was replaced on the lip of the syringe. 2-5 ml of native binding buffer with 0.02% Sodium Azide was poured into the syringe and both ends were wrapped in parafilm. The reusable column was stored at 4°C.

Purification under Native conditions using Qiagen Ni-NTA Spin Kit

Native Lysis Buffer B was used.

The spin columns were equilibrated using 600 µL of Lysis Buffer B, centrifuged at 2900 rpm and the buffer was discarded. 600 µL of supernatant was loaded onto spin column, centrifuged for 5 minutes at 1600 rpm and supernatant was collected for SDS PAGE analysis. Spin columns were washed with 600 µL Native wash buffer B and centrifuged at 2900 rpm twice and washes were collected for SDS PAGE analysis. 300 µL Elution buffer was loaded onto spin column then centrifuged at 2900 and this was repeated three times. 20 µL samples of the elutions were taken for SDS PAGE analysis.

Protein preparation under denaturing conditions

Frozen protein pellets were thawed on ice for 15 minutes then resuspended in Denaturing Buffer B at 5 ml per gram weight. Protein solutions were incubated at 25°C with shaking for 1 hour, then centrifuged at 10,000 rpm for 20-30 minutes at 25°C. The supernatant was saved for purification.

Protein purification under denaturing condition using Qiagen NI-NTA Spin Kits

The spin columns were equilibrated using 600 µL of denaturing Buffer B, centrifuged at 2900 rpm and the buffer was buffer was discarded. 600 µL of supernatant was loaded onto spin column, centrifuged for 5 minutes at 1600 rpm and the supernatant was collected for SDS PAGE analysis. Spin columns were washed three times with 600 µL of Denaturing Buffer C, centrifuged at 2900 rpm and washes were collected for SDS PAGE analysis. 300 µL of Denaturing Buffer E was loaded onto the spin column

and allowed to settle for 1 minute. The spin column was then centrifuged at 2900 and the elution was kept in an Eppendorf. 5-6 Elutions were collected and 20 µL of each sample was kept for SDS PAGE analysis.

Protein refolding for purification under denaturing conditions

Protein was dialyzed into 5 Liters of Vesicle Buffer, with gradually decreasing urea concentrations over 2 days.

SDS PAGE Analysis

A 10% SDS-PAGE Gel was made up as follows:

Resolving gel

2.55 ml dH_2O, 3.75 ml 1.5M TRIS pH 8.7, 100µL of 10% SDS, 3.2 ml of 30% Sigma Aldrich Acrylamide/Bis-acrylamide, 100µL Aps and 15 µL TEMED.

Stacking gel

7ml dH_2O, 1.25 ml 1M TRIS pH 6.8, 50 µL of 10% SDS, 1.7ml of 30% Sigma Aldrich Acrylamide/Bis-acrylamide, 50 µL APS and 15 µL TEMED.

Both gels were set in the 37 °C incubator.

2.2.5 – Vesicle Protocols

DLS

We used the Malvern Zetasizer Nano DLS and program, all DLS experiments were run in Vesicle Buffer A at 25ºC.

For Vesicle controls

1.1ml of vesicles was pipetted into the DLS cuvette and measured using the Malvern Nano program.

For Vesicles with protein

1 ml of vesicles and 100 µL of protein were pipetted into the DLS cuvette and measured using the Malvern Nano program.

Vesicle Preparation by Extrusion

Preparation of Vesicles

Lipids were weighed to make up 1 mM lipid suspensions and chloroform to the appropriate volume was added. Lipid suspensions were dried on a rotary evaporator at 20°C until all the chloroform had evaporated then placed on a vacuum line to remove any remaining chloroform. Lipids were rehydrated with the appropriate volume of

Vesicle Buffer A to make a 1mM solution then bath sonicated, ensuring all the lipid has been removed from the bottom of the flask. Nine freeze-thaw cycles were then carried out using liquid nitrogen and a room temperature water bath. If storing the lipid for later use, do not complete the last thaw cycle.

Extrusion

The lipid solution was allowed to stand at room temperature for 30 minutes then using Avanti's Extrusion kit, vesicles were pushed through 200 nm membrane and placed in a glass vial.

2.2.6 – Stopped Flow Protocol

All kinetic experiments were conducted in Vesicle Buffer A at 20℃. Measurements were performed with a High-Tech Scientific stopped flow system. The concentrations stated are those before mixing in the stopped flow observation cell. All stopped flow traces were analyzed by TgK (Kinetic Studios). Cerulean fluorescence was measured by excitation at 436 nm and Light scattering was measured at 545 nm using the GG-455 optical filter. The time-dependent data were best fit to a double exponential function showing two distinct phases of the reaction; a rapid initial phase and a second, more gradual phase

2.2.7 - NI-NTA Magnetic Bead Assay

Ni-NTA Magnetic Agarose Beads from Qiagen were used for this assay.

Protein binding

The magnetic beads were resuspended in the manufacturer's buffer then placed immediately on a magnetic separator and the buffer was carefully removed using a pipette. The beads were then re-suspended in 1 ml of Vesicle Buffer A, mixed thoroughly and placed on the magnetic separator. The buffer was again removed and the beads were resuspended in 1 ml Vesicle buffer A. This was repeated once more and then the Agarose bead solution was mixed thoroughly by vortexing for 20s. Immediately, 250 µL of the Agarose bead solution was pipetted into 4 separate 1.5ml eppendorfs. 250 µL of the TH1 protein in Vesicle Buffer A was added to 3 of the eppendorfs with 500 µL of Vesicle Buffer A to make up a total volume of 1 ml. A negative control was set up by adding 750 µL of Vesicle Buffer A to the agarose bead solution in one of the eppendorfs. All 4 eppendorfs were incubated with stirring at 4°C for 1 hour to ensure the protein was bound to the agarose beads. The solutions were thoroughly mixed by vortexing once again and then placed on the magnetic separator. All of the buffer was removed carefully, with the unbound protein and saved in separate Eppendorf tubes. The magnetic beads were washed through with Vesicle Buffer A twice, placed on the magnetic separator and the solution was removed.

500µL of vesicles suspended in Vesicle Buffer A were added along with 500µL of the buffer to make up a total volume of 1 ml and mixed thoroughly. The eppendorfs were incubated on a 4℃ shaking stirrer overnight, to allow time for the vesicles to bind to the protein. The solution and beads were separated using the magnetic separator and then the solution was removed and pipetted into a separate Eppendorf. The beads were then washed through with Vesicle Buffer A.

FM464 Analysis

50 µL of FM464, a lipophilic fluorescent dye, was then added to each Eppendorf and then thoroughly mixed. The dye was then allowed to bind to the vesicles for 30 minutes, then mixed once again and placed on a magnetic separator. The solution was taken out and saved, then the beads were washed twice with Vesicle Buffer A, then washed with 500µL Elution buffer twice to remove the protein. The elution buffer solutions were placed into a 1 ml cuvette and compared visually, any color change was noted and saved for a fluorescence scan to accurately detect any dye remaining in the solutions that wasn't visible.

2.2.8 - Microscopy

Samples were visualized using an Olympus IX71 microscope

Standard Protocol

A 2% Agarose solution was melted as 95°C, then 50µL was pipetted onto a microscope slide, using a pro former to create a flat surface. Up to 20µL of samples were mounted on the agarose pads and allowed to dry slightly so as to mobilize them. A coverslip was gently placed and secured on top of the agarose pad and then samples were visualized using the Olympus IX71 microscope.

SRB Red

A 2% Agarose solution was melted at 95°C hot plate and a 1.5ml Eppendorf was filled with water and kept at 37°C. Once melted, the agarose was quickly diluted to 0.5% and the Eppendorf was kept at 37°C so it stayed molten. 0.01% SRB Red was made up and added to the molten 0.5% agarose then pipette mixed carefully. 15 µL of the SRB-agarose was mixed into 500 µL of vesicles and 20µL of the agarose mix was pipetted onto a microscope slide and allowed to set. A cover slip was gently placed over the top of the agarose and secured, then vesicle samples were visualized using the Olympus IX71 Microscope using the appropriate filters.

2.2.9 - Sedimentation Assay

5µL of DPPE, DSPG and POPC vesicles were added into three separate 1.5ml eppendorfs. 40µL of Vesicle Buffer A and 5µL of TH1 protein were pipetted into each of these eppendorfs to make a total volume of 50µL. A protein control containing 5µL of TH1 protein and 45µL of Vesicle Buffer A was also set up and labelled. Eppendorfs were centrifuged at 10k for 30 minutes. The supernatant from each Eppendorf was

removed carefully and placed into a separate clearly labelled Eppendorf. The pellet was resuspended into 50µL of Vesicle Buffer A. 10µL of protein loading buffer was added to each of the 8 tubes. These were then run on a 10% SDS-PAGE gel for 60 minutes and placed into coomassie stain and imaged once destained

Chapter 3

Results

3.1 – Hum-1 TH1

3.1.1 – Cloning of the TH1 Domain

Initially, we needed to determine whether the TH1 domain and phospho-mutant were soluble and could be purified. If these proteins were expressing as expected then we would see a band at 27.5kDa on an SDS PAGE gel. Initially we used *E. coli* BL21 De3 cells for expression, however, there was very little expression when the protein was induced with this strain (Figure 8A).

In response to the lack of expression, we transformed our plasmids into BL21 Rosetta Pduet Cam 1 cells; a chloramphenicol resistant strain that co -expresses Calmodulin. As expression using this strain was successful (Figure 8B), the next step was to determine the best way to purify the protein.
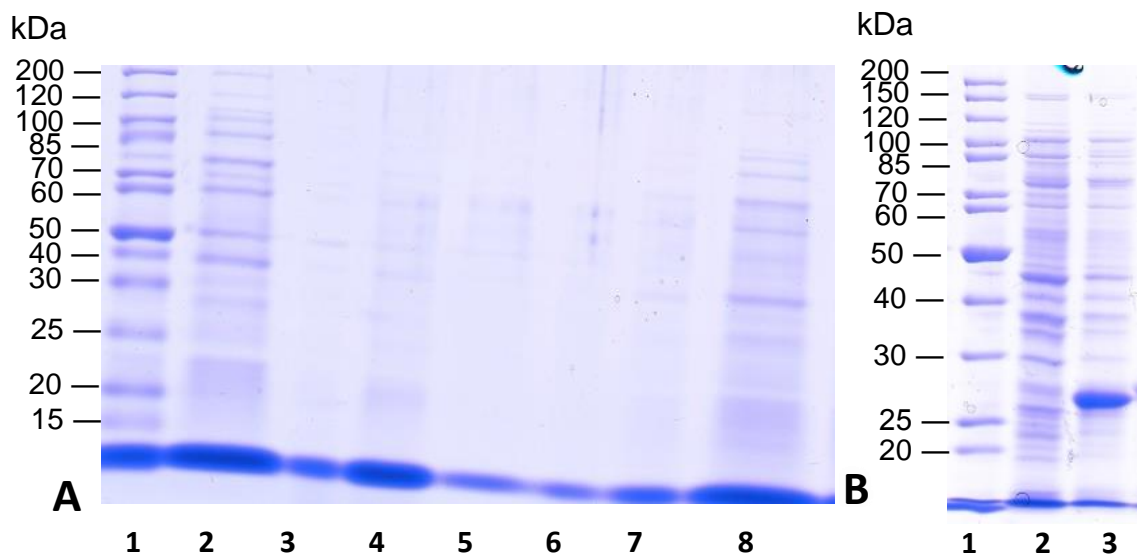

Figure 8: Hum_1 TH1 expression. SDS PAGE gels were used to determine the success of protein inductions. **A.** TH1 expression using *E. coli* BL21 DE3. *(Lane 1)* Protein ladder, *(Lane 2)* Pre-induction sample, *(Lanes 3-7)* empty lanes, *(Lane 8)* post induction sample. Band expected at 27.5kDa, however there was no expression shown after a standard induction. **C:** TH1 expression using *E. coli* BL21 Cam-1 pLysS. *(Lane 1)* Protein ladder. *(Lane 2)* Pre-induction sample *(Lane 3)* Post induction sample. Band expected at 27.5kDa; there is considerably more expression with this strain after a standard induction.

3.1.2 - TH1 Purification

We started off by attempting purification under native conditions using a cobalt column. However, we discovered that a lot of protein was lost during purification, and when samples from each purification stage were run on an SDS PAGE gel, we realized that the protein was being lost in when it was loaded onto the column. This meant that the His-tag on the protein was not binding to the column. We then attempted to use a nickel column, however the same result was observed (Figure 9A). Since the protein was being expressed as normal, and assuming the His-tag was intact, we hypothesized that the protein might have been binding to the membrane lipids in the cells so was being lost during centrifugation. To confirm this, we purified the protein under

denaturing conditions, so that if the His-tag was damaged during one of the stages, the purification would fail, however if the protein was binding to lipids or other cell components in the cell, then this purification method would be successful. Therefore, we used this method for purification and our hypothesis was confirmed (Figure 9B) and the purification was successful. The protein was seen between 20 and 25 kDa, however this may be because while the protein is denatured it can travel easier through the gel, furthermore SDS gives a relative molecular mass rather than a true molecular mass so we determined that this was our protein. We then dialyzed the protein from the 8M urea elution buffer to Vesicle Buffer A, however, the protein quickly precipitated out of solution even with a slow dialysis, so we kept the protein in the urea buffer. This limited the experiments we could carry out with the protein, as the urea buffer would have denatured the protein, so any interactions could have been affected by this.
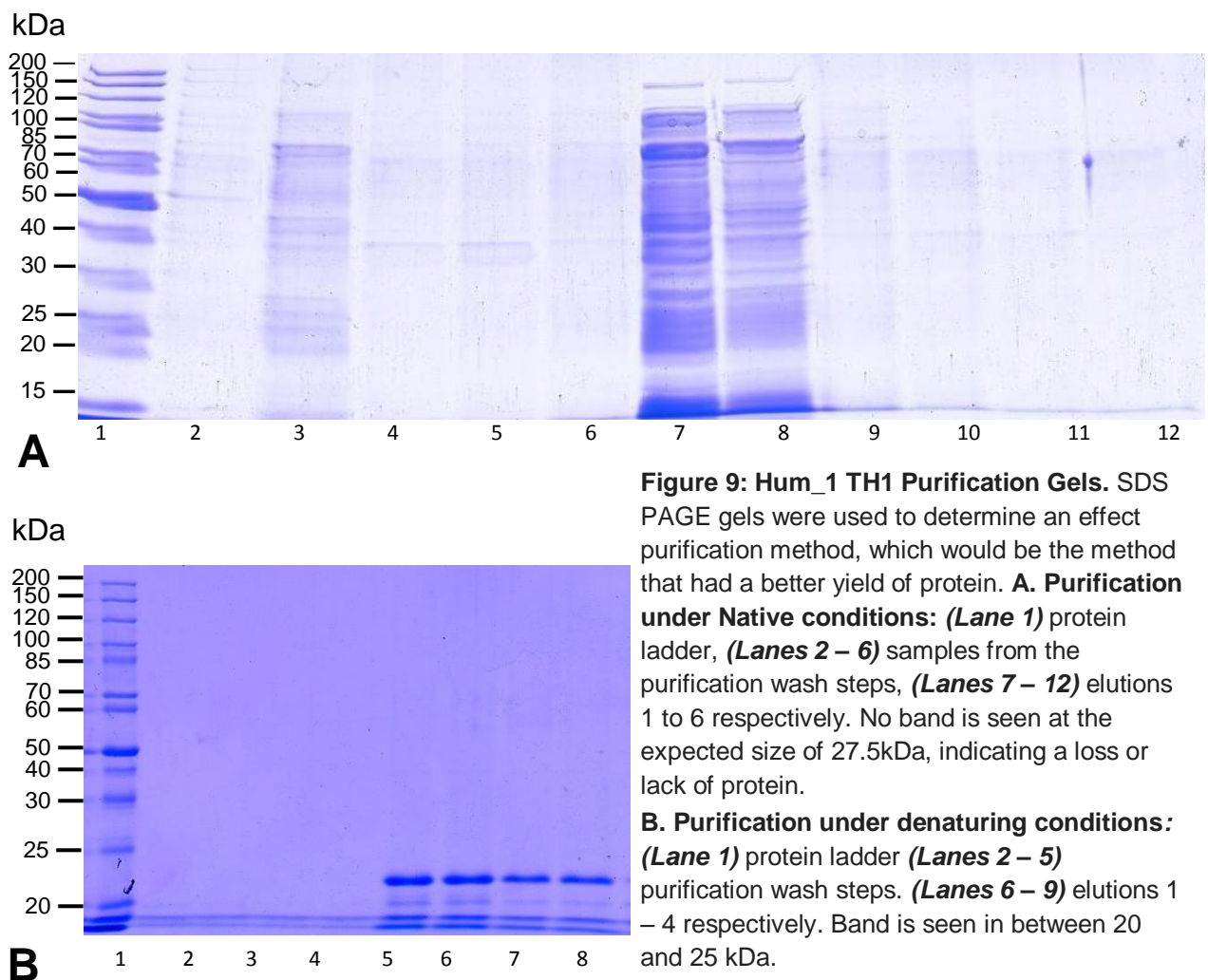

Figure 9: Hum_1 TH1 Purification Gels. SDS PAGE gels were used to determine an effect purification method, which would be the method that had a better yield of protein. **A. Purification under Native conditions:** *(Lane 1)* protein ladder, *(Lanes 2 – 6)* samples from the purification wash steps, *(Lanes 7 – 12)* elutions 1 to 6 respectively. No band is seen at the expected size of 27.5kDa, indicating a loss or lack of protein.

B. Purification under denaturing conditions: *(Lane 1)* protein ladder *(Lanes 2 – 5)* purification wash steps. *(Lanes 6 – 9)* elutions 1 – 4 respectively. Band is seen in between 20 and 25 kDa.

3.1.3 – Sedimentation assays to determine TH1 lipid binding properties

Following this, we carried out some simple sedimentation assays using the purified TH1 domain, in order to determine the phospholipids that it interacts with and how that differs from the phospho-mutant. Sedimentation assays are assays based on the

sedimentation of vesicles and bound proteins when centrifuged [53]. If the protein binds to the lipid vesicles, both sediment to the bottom of the tube, forming a pellet that can be analyzed by running on an SDS PAGE gel.

Initially we ran the TH1 with DSPG, DPPE and POPC vesicles, however, when run on an SDS PAGE gel, no difference between the three was observed (Figure 10A). We then set up a control of the protein alone to ensure that the protein did not sediment when centrifuged alone. We carried out this experiment at 4 centrifugation speeds; 2000, 5000, 7500 and 10000 rpm. The supernatant was then removed and both the supernatant and pellet were analyzed using SDS PAGE. The protein was found in the pellet (Figure 10B). We repeated this, and observed the same result and thus concluded that we could not use sedimentation assays for this protein. Some membrane binding proteins tend to oligomerize or aggregate, which leads to sedimentation when centrifuged [53], which could be a possible reason for this assay being unsuccessful for the TH1 domain.
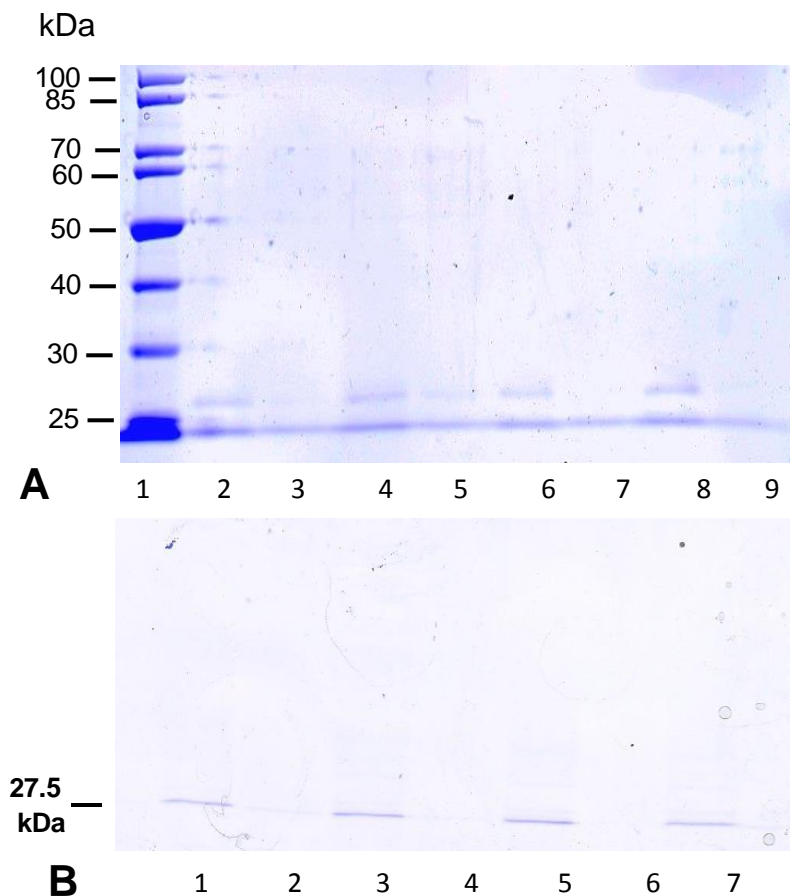

Figure 10: SDS PAGE gels from the sedimentation assay. **A. Sedimentation assay** with POPC, DSPG and DPPE lipid vesicles showing the pellets and supernatants. *(Lane 1)* Protein ladder *(Lane 2)* Negative control pellet *(Lane 3)* Negative control supernatant *(Lane 4)* POPC pellet *(Lane 5)* POPC supernatant *(Lane 6)* DSPG pellet *(Lane 7)* DSPG supernatant *(Lane 8)* DPPE pellet *(Lane 9)* DPPE supernatant. **B. Sedimentation assay negative control.** Protein spun without phospholipid. *(Lanes 1, 3, 5 & 7)* Protein pellet samples run at 2000, 5000, 7500 and 10000 rpm respectively *(Lanes 2, 4 & 6)* Protein supernatant samples when run at 2000, 5000 and 7500 rpm respectively. At all speeds the protein sedimented into the pellet.

3.1.4 – Agarose Bead Assay to determine TH1 lipid binding properties

Following the results of the sedimentation assays, we decided to use Qiagen's Ni-NTA Magnetic Agarose Beads for a TH1 binding assay. We chose to do this as the His-tag on the protein can bind to the nickel coated agarose beads, and when placed on a

magnetic separator, the magnetic beads and bound protein would be attracted to the magnet, and the unbound protein could be removed. When the lipid vesicles were added, if they bound to the protein, a bead-protein-vesicle complex could be formed, and again the unbound vesicles could be separated and removed, leaving only the bound protein and vesicles. FM4-64, a lipophilic dye that would bind to the vesicles, was added to the protein samples to determine whether vesicles were present, which would tell us whether the TH1 interacted with any of the lipids. Figure 11 below is an image of the results from the FM464 analysis. Due to time constraints, we were unable to complete a full scan of each sample, which would have allowed us to determine whether there was FM464 present in each sample, thereby allowing us to determine the lipids that the protein interacts with. Quantification of FM464 in samples would allow us to accurately determine this as we were unable to do so visually.
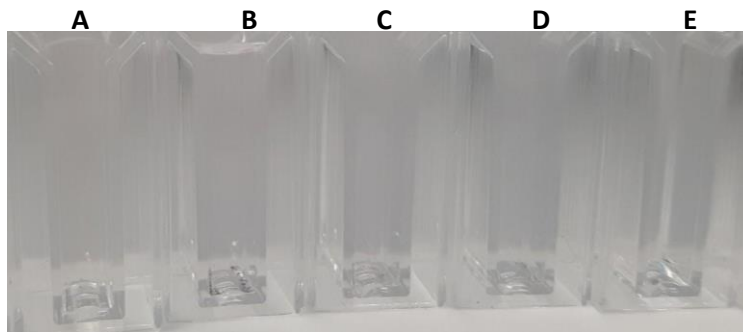
Figure 11. Samples from the Agarose Bead Assay. Cuvettes containing Hum-1 TH1 with *(A)* DSPG, *(B)* DPPE, *(C)* POPC, *(D)* Negative control, *(E)* Vesicle Buffer A. Little visual difference observed.
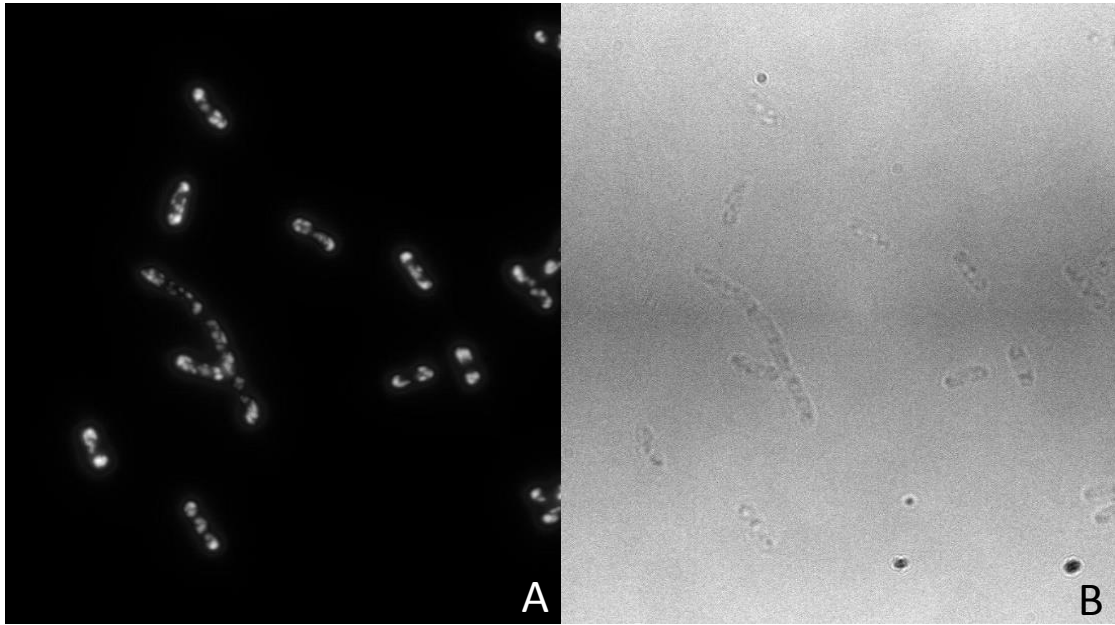
3.1.5 – Neon Green tagged TH1

As we were only able to purify the TH1 domain under denaturing conditions, we decided to visualize where it was localizing so as to determine whether this was due to it being bound to phospholipids or was localizing in the periplasmic space. We created a neon green TH1 wild type and Phospho-mutant so that we would be visible under a microscope and we could then potentially use this protein with other techniques, such as stopped flow, to determine its lipid interactions.

As with the original TH1 and Phospho-mutant, expression was carried out in BL21 Cam-1 cells until we had reached an optical density of 0.4. We then took 20µL of the cell culture and pipetted them onto an agarose pad on a microscope slide. Finally we visualized and imaged the cells under the microscope (Figures 12 & 13).

The images revealed to us that the wild type TH1 domain was localizing in inclusion bodies at the poles of the cells (Figure 12), whereas the phospho-mutant was predominantly cytoplasmic (Figure 13). This difference in localization suggested that phosphorylation of TH1 may play a role in its localization. Further investigation into this would need to be carried out in order to fully understand this.

Figure 12: Microscopy images of wild type Neon Green tagged Hum 1 TH1 expression in BL21 Cam 1 cell. (A) Fluorescence image **(B)** Phase image. Fluorescence images show localization in inclusion bodies rather than in the cytoplasm.
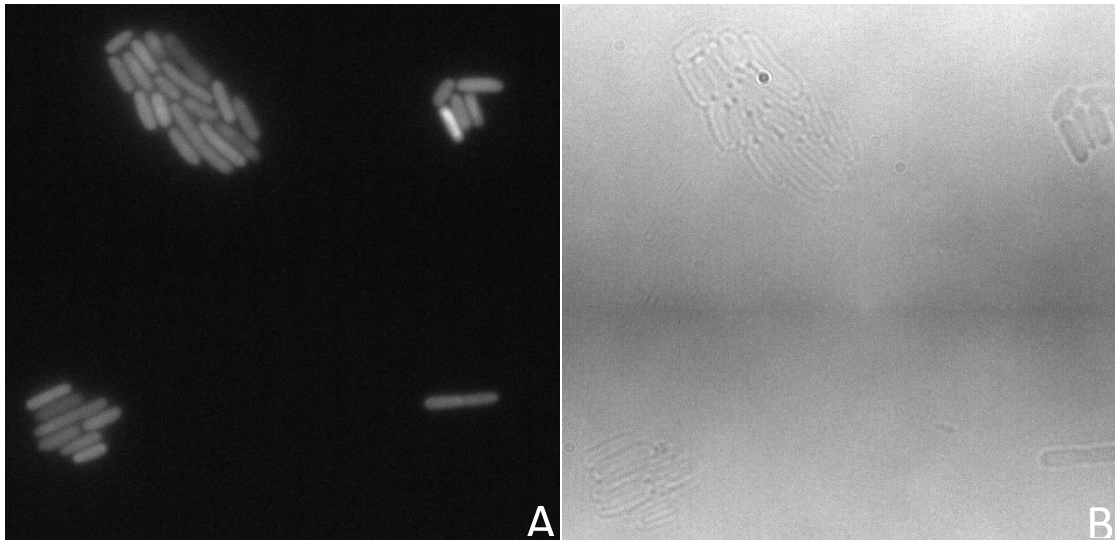
Figure 13: Microscopy images of Neon Green tagged Hum 1 TH1 phospho-mutant expression in BL21 Cam 1 cells. (A) Fluorescence images **(B)** Phase images. Fluorescence image shows localization in the cytoplasm rather than around membranes or in inclusion bodies.

3.2 - Alpha Synuclein and its phospholipid interactions

The next part of the project was to investigate how αSynuclein interactions with different phospholipids and determine whether its acetylation had any impact on these interactions. The acetylated and un-acetylated αSynuclein used were cloned, expressed and FPLC and His-tag purified by another member of the lab.

3.2.1 – DLS Experiments

Dynamic light scattering is a technique used to study the behavior of molecules in solution [54]. A sample is exposed to a monochromatic light source such as a laser and a detector detects the light scattered by the sample, allowing us to determine the size profile of the sample [54]. We used unilamellar vesicles in the DLS to determine whether the protein interacted with the vesicles by adding αSynuclein to a solution of uniform vesicles. A negative control was initially taken so as to eliminate any changes that are solely due to the addition of protein, and we could observe the effect on the phospholipids only.

DPPE

While preparing vesicles made from this lipid, we discovered that it was highly unstable. Due to its hydrophobic nature, the lipid would form a layer along the top of the buffer rather than forming vesicles within the buffer. After sonication, we were able to dissolve some of the lipid, however after a short period of time, it would begin to precipitate out of solution and form a layer once again. When run through a DLS alone the data was inconsistent with each run (Figure 14A), in comparison to POPC vesicles that would produce the same reading with each run (Figure 14B) so as a result of this, we did not use this lipid in DLS experiments with αSynuclein until we could suspend them in solution completely.
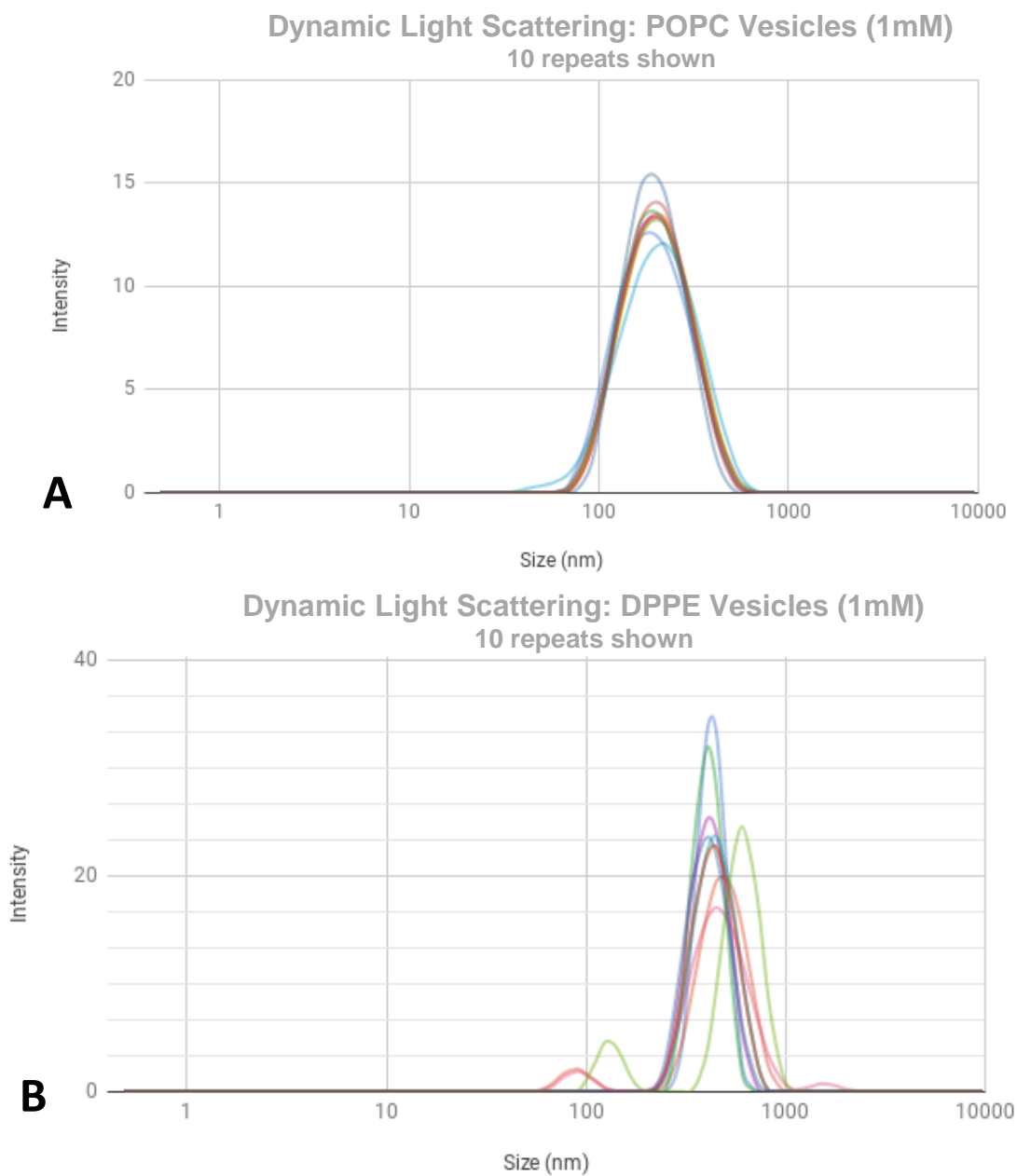
Figure 14: DLS Size-Intensity plots of vesicles in Vesicle Buffer A: *(Graph A)* Stable POPC vesicles that are ~ 100nm. Each repeat is consistent. *(Graph B)* DPPE vesicles in *Vesicle buffer A.* Inconsistent readings; vesicles of different sizes within the sample and also larger than expected at ~500-600 nm.

POPC formed stable vesicles that were ~100 nm in size (Figure 15), shown by a single peak slightly larger than 100 nm on an Intensity-Size plot. (This would appear slightly larger due to the hydrodynamic radius; the water molecules surrounding the vesicles). When acetylated αSynuclein was added, there was no significant change to the vesicles, on the other hand when un-acetylated αSynuclein was added, a slight broadening of the peak was seen, suggesting a greater size distribution (Figures 16A-16B). However, this change could be due to the addition of protein. We then allowed the proteins to interact with the vesicles for 30 minutes and ran them through the DLS. For both un-acetylated and acetylated, two peaks were seen; one at 100 nm with a wider distribution and the other at 5000 nm (Figures 17A & B). The absence of intermediate sized vesicles suggested that the vesicles had formed aggregates rather than increasing in size. This was consistent when repeated.
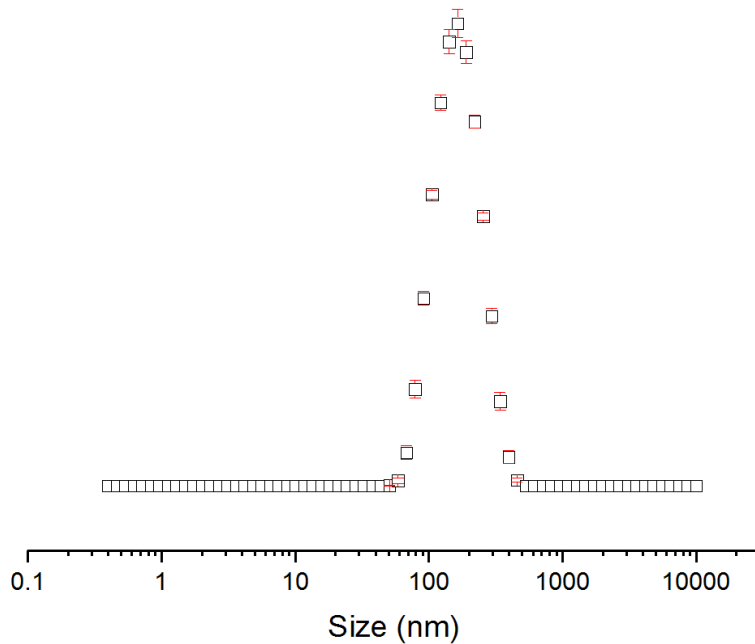
Figure 15: DLS size-intensity Graph. POPC Vesicles in *Vesicle Buffer A* showing an average size of 100nm, as expected. An average of 10 readings is shown.

POPC vesicle and Acetylated αS
Average of 10 readings shown

A

POPC vesicles and Un-acetylated αS
Average of 10 readings shown

B
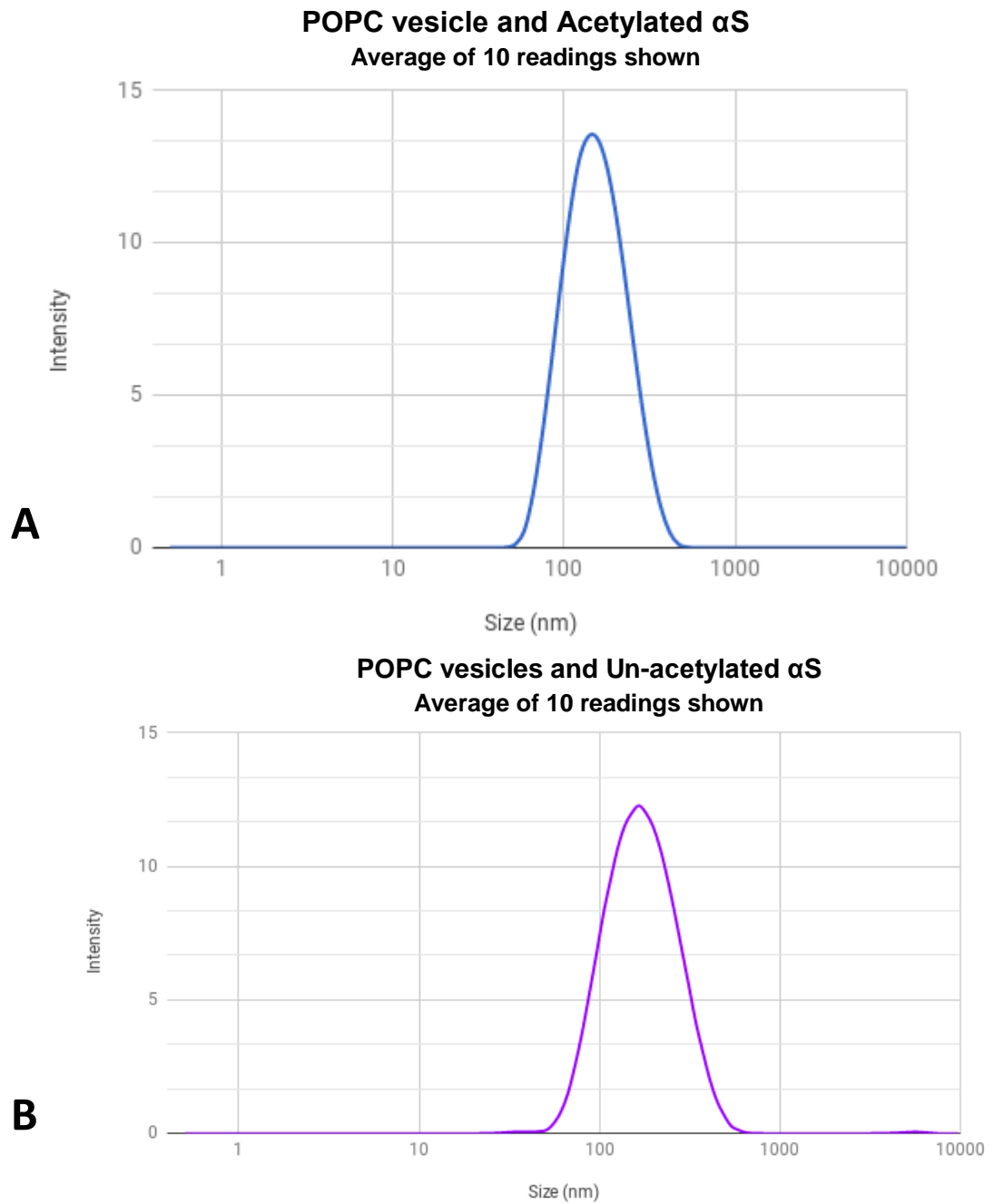
Figure 16: Size-intensity plots of POPC vesicles (Average of 10 runs) with (A) Acetylated αSynuclein showing little change in size and **(B)** un-acetylated αSynuclein, showing a slight broadening which indicated a greater size distribution.

POPC and Unacetylated aS after 30 minutes (Average)
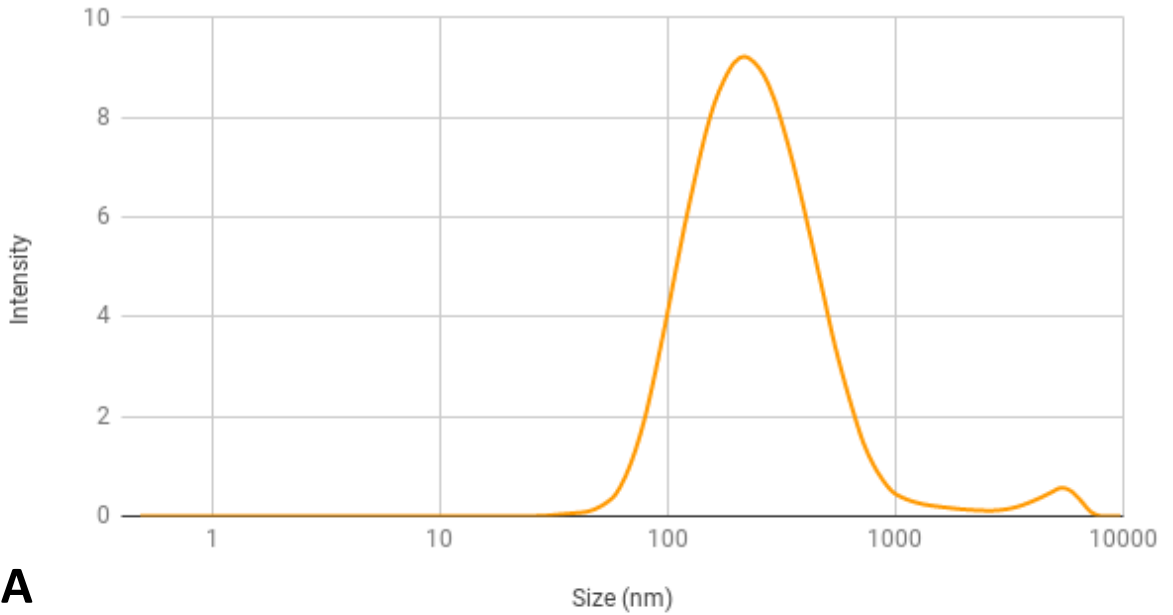
POPC and Acetylated Alpha Synuclen
After 30 minutes (Average)
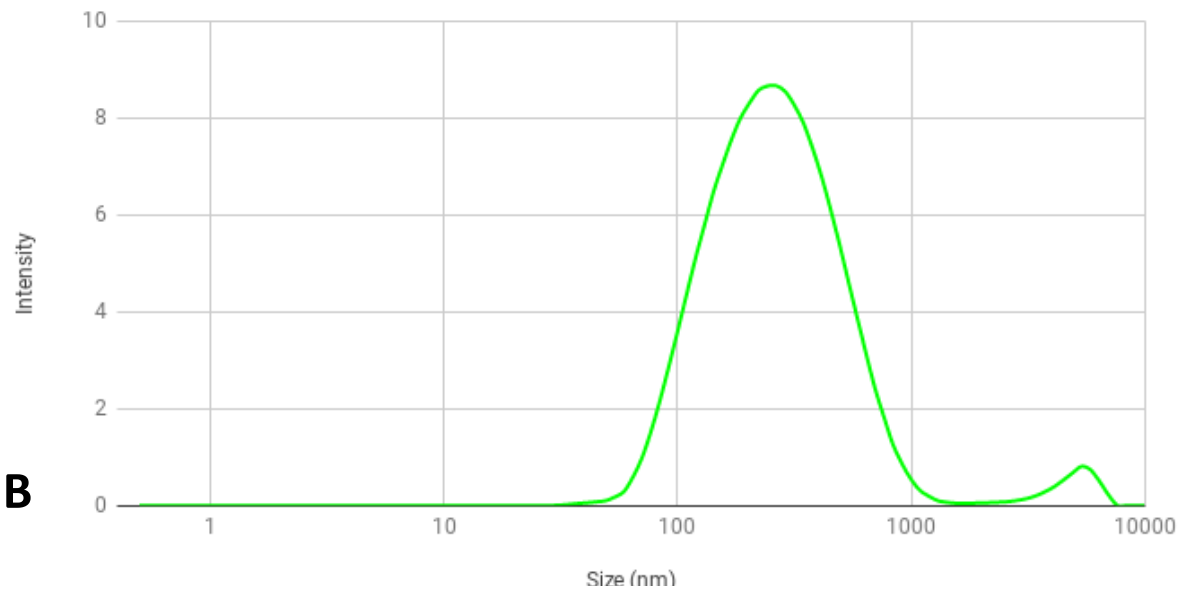
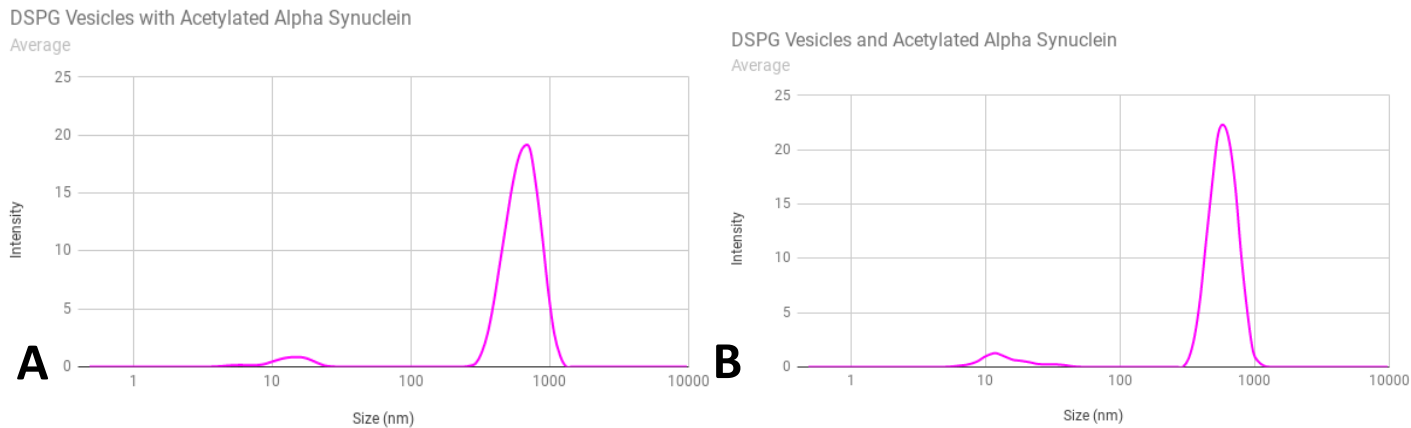**Figure 17: Size intensity plots of POPC** vesicles (Average of 10 runs) after 30 minutes of incubation with (A) un-acetylated αSynuclein and (B) acetylated αSynuclein. Both showing a slight increase in size and larger species at 5000nm, suggesting aggregation. Both also show a broadening of the size/intensity peaks, indicating a larger size distribution within the sample.

.

DSPG vesicles formed vesicles ~200 - 300 nm and had a tendency to form aggregates naturally; shown by two consistent peaks on an intensity-size plot - one at ~200 nm and the other at 5000 nm (Figures 18). Although multiple peaks were present with DSPG vesicles, this was consistent through all readings, so we were able to use them in DLS analysis. When acetylated αSynuclein was added to the vesicles, two peaks were consistently seen; one at ~ 600 nm and the other at ~13 nm (Figure 19). The peak at ~ 600 nm was roughly twice the size of the normal DSPG vesicles, potentially suggesting increased aggregate formation. The smaller vesicles, however, may have been lipid that could have been broken down from the larger aggregates and re-formed into smaller vesicles. Another possible explanation could be that the vesicles had been fused together by the acetylated αSynuclein, however the absence of intermediate sizes or gradual changes suggests that this may not be the case. As there was a difference in intensity-size plots for POPC when run after 30 minutes compared to being immediately run, we then decided to monitor the interaction on the DLS by running the DSPG vesicles with acetylated αSynuclein repeatedly 100 times. This would allow us to see gradual changes in size, and may give an indication as to whether the acetylated αSynuclein was increasing DSPG aggregation or increasing DSPG size. After 100 runs, the same two peaks were consistently seen on the Intensity-size plots (Figures 19A-19B). This suggests increased aggregate formation rather than increased size, however further experiments or microscopy would need to be conducted to confirm this.
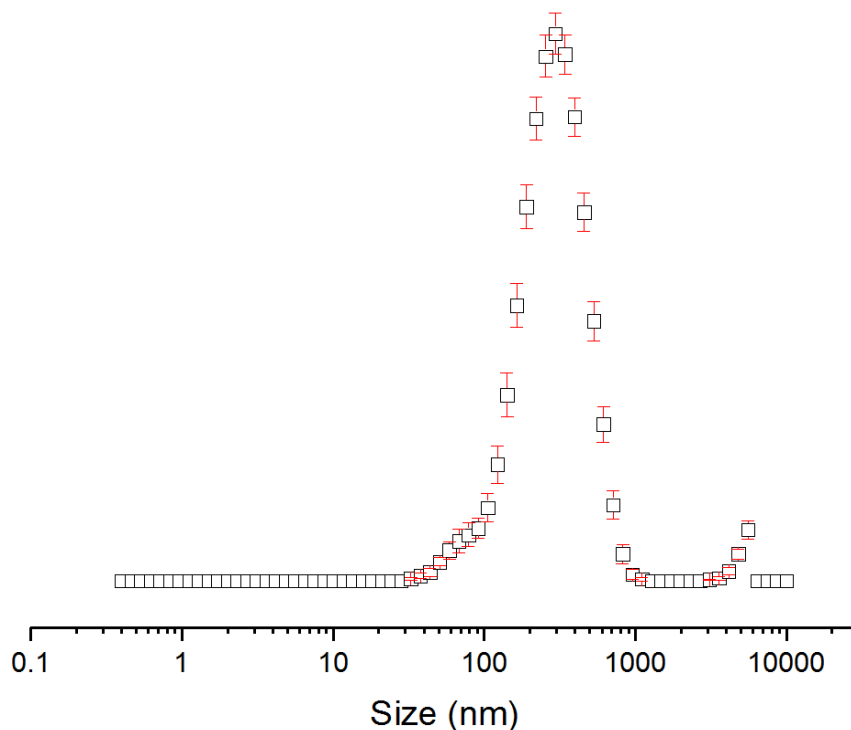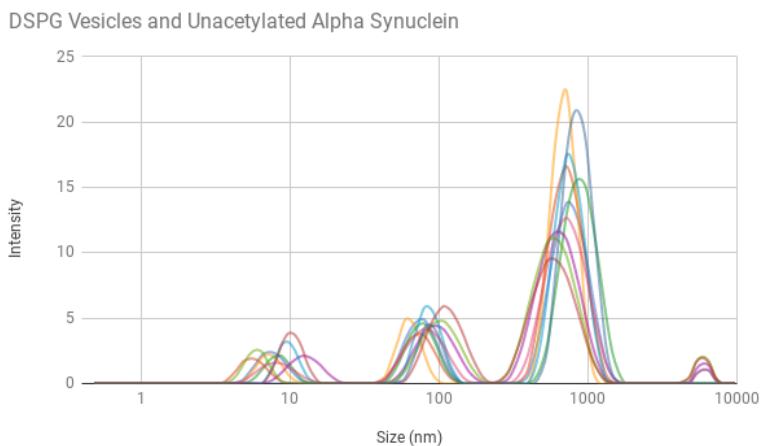
Figure 18: Size-intensity plot of DSPG vesicles alone in vesicle buffer A (Average of 10 runs). Average size of species in this sample is 200 nm and a small peak at 5000 nm may suggest aggregate formation.
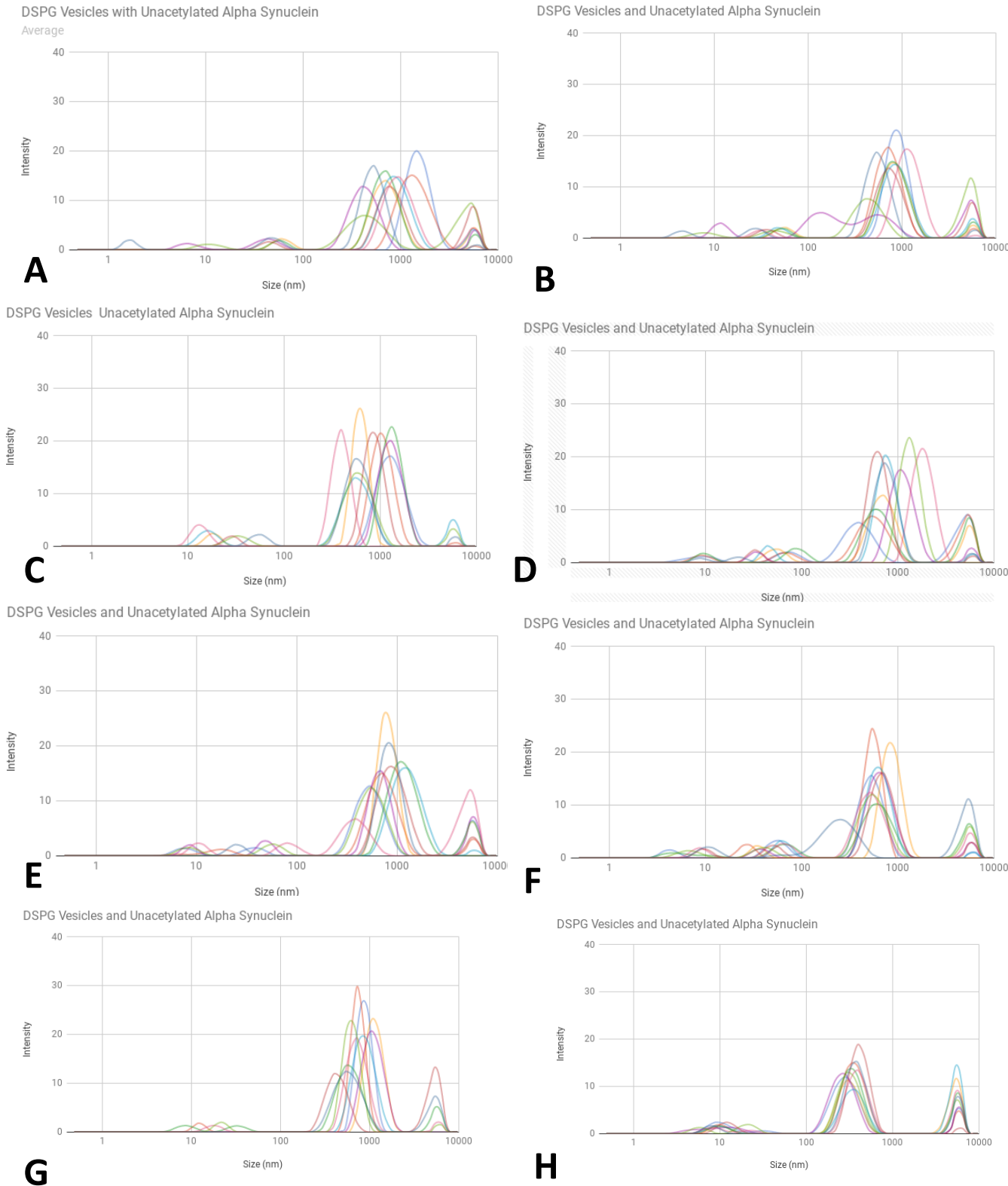
DSPG Vesicles with Acetylated Alpha Synuclein
Average

A

DSPG Vesicles and Acetylated Alpha Synuclein
Average

B

Figure 19: Size-intensity plots of DSPG vesicles with acetylated αSynuclein: (A) Average of 10 runs. **(B)** After 100 runs. An increase in size is observed and maintained after 100 runs.

We then carried out the same DLS experiment with the un-acetylated αSynuclein. After one run, multiple peaks were seen on the intensity-size plot (Figure 20) indicating different sized vesicles. As with the acetylated αSynuclein, we ran these on the DLS 10 times (creating 100 individual readings). And plotted intensity-size graphs (Figures 21 A-H). The vesicles appear to increase in size, until they reach 5560 nm, at which point they burst. We hypothesize that the lipids from these large vesicles are either incorporated into the other vesicles or they reform into small vesicles that begin to fuse again. When following a single peak along, we can see this pattern more clearly (Figure 22); vesicles of various sizes appear to be fusing to form larger vesicles and bursting at 5000 nm. This result prompted us to begin imaging the vesicles and visualize their interaction with αSynuclein.

DSPG Vesicles and Unacetylated Alpha Synuclein

Figure 20: Size intensity plot of DSPG vesicles with un-acetylated αSynuclein. Multiple peaks at 10 nm, 100 nm, 1000 nm and 5000 nm are observed.

Figure 21: Size intensity plots of DSPG vesicles with un-acetylated αSynuclein monitored over 100 runs. Each graph showing 10 individual runs, each set of 10 consecutively starting from graph **A** to graph **H**. Vesicles appear to be growing in size until 5000 nm then re-forming to make smaller vesicles.
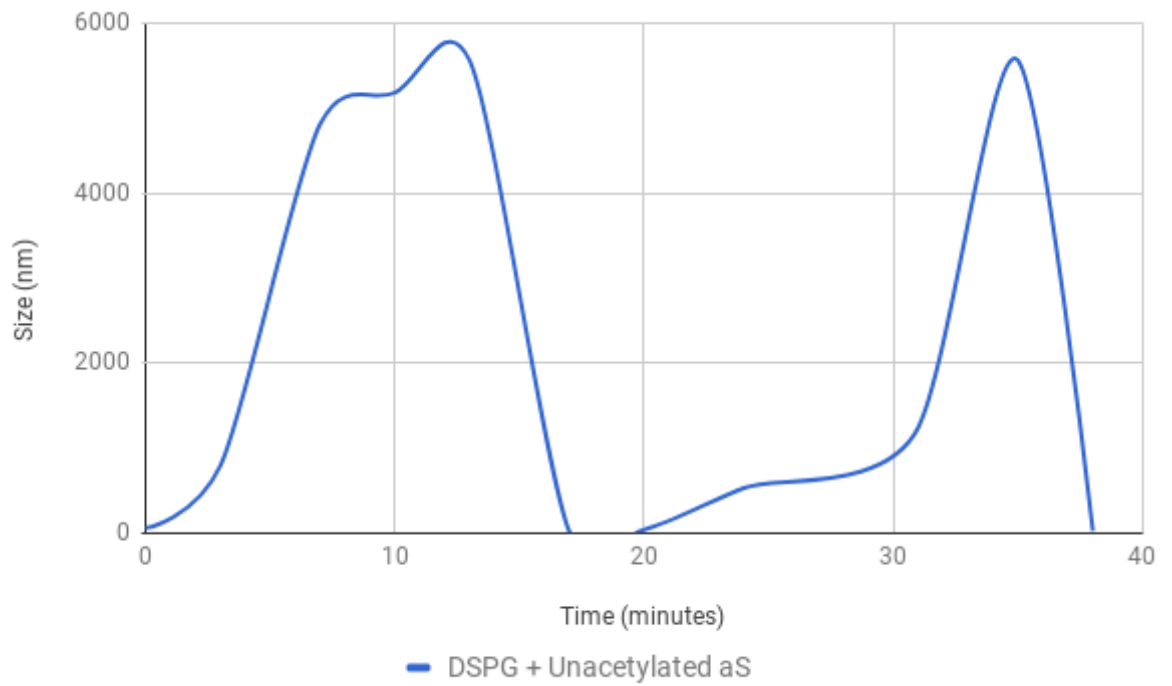
Figure 22: Vesicle size (nm) monitored over time (minutes). Vesicles appear to be growing in size until they reach ~5000 nm (5 microns), at which point they burst and reform into smaller vesicles, then begin to grow in size once again.

3.2.2 – Microscopy using Synthetic vesicles

We began to investigate the different ways to image the vesicles so that we could visualize their interaction with αSynuclein. Initially we used the agarose pads for imaging the vesicles, however we were unable to take clear images due to the motility of the vesicles and their small size (~100-200 nm) made it difficult to differentiate between the agarose cracks and the vesicles. We then decided to use SRB Red, a fluorescent dye, to image the vesicles, as described by Lira R. B. et al 2016 in *"Posing for a picture: Vesicle immobilisation in agarose gel"* [55]. The images were not as expected, the dye was being taken into the vesicles and make them fluorescent, and which made it difficult to distinguish between the fluorescence of the agarose and the vesicles. Due to this, we were unable to obtain clearer images of the vesicles (Figure 23). The vesicles with acetylated DSPG, as with the other lipids, were too small to image, even with SRB Red.
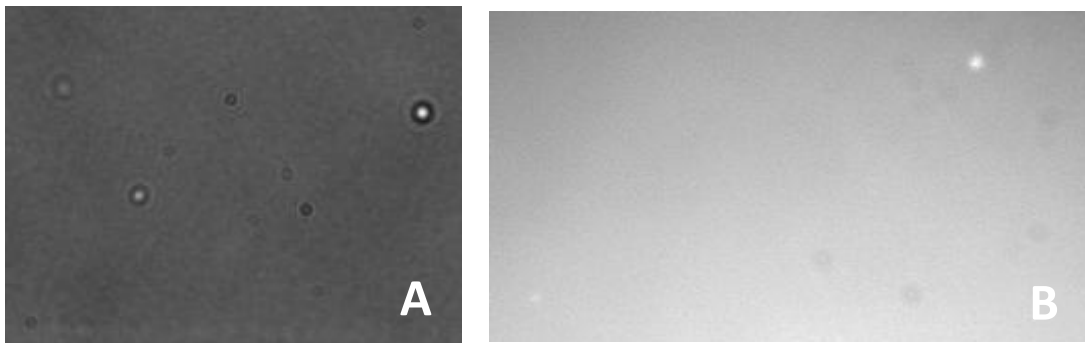
Figure 23: Microscope images of DSPG Vesicles with Un-acetylated αSynuclein. **(A)** Phase Images Vesicles were too small to distinguish. As there were holes within the agarose, so we were unable to obtain clearer images. **(B)** SRB Red fluorescence; some vesicles would take up the fluorescent compound, however there would also be spots of brightness within the agarose, so we were able to differentiate between vesicles and agarose fluorescence. Therefore, we were unable to determine any effect of αSynuclein on the vesicles.

3.2.3 - Stopped Flow Spectroscopy using Alpha Synuclein

Stopped flow is a technique used to measure immediate kinetic changes that occur when two molecules interact with one another. We decided to use this technique as it would allow us to see any change to the vesicles when αSynuclein was rapidly mixed with the vesicles. We used the vesicles made up of the DSPG phospholipid, as they reacted the most with un-acetylated αSynuclein. We also tested αSynuclein at different concentration to determine whether concentration had an impact on these interactions. This was done as in previous experiments by other members of the lab, the concentration of αSynuclein has greatly impacted interactions with cellular membranes.

We used a Bradford assay, according to the manufacturer's instructions, to compare the concentrations of the stock acetylated and un-acetylated αSynuclein (Figure 24), which revealed that their protein concentrations were similar, however un-acetylated αSynuclein was slightly higher (Table 2).
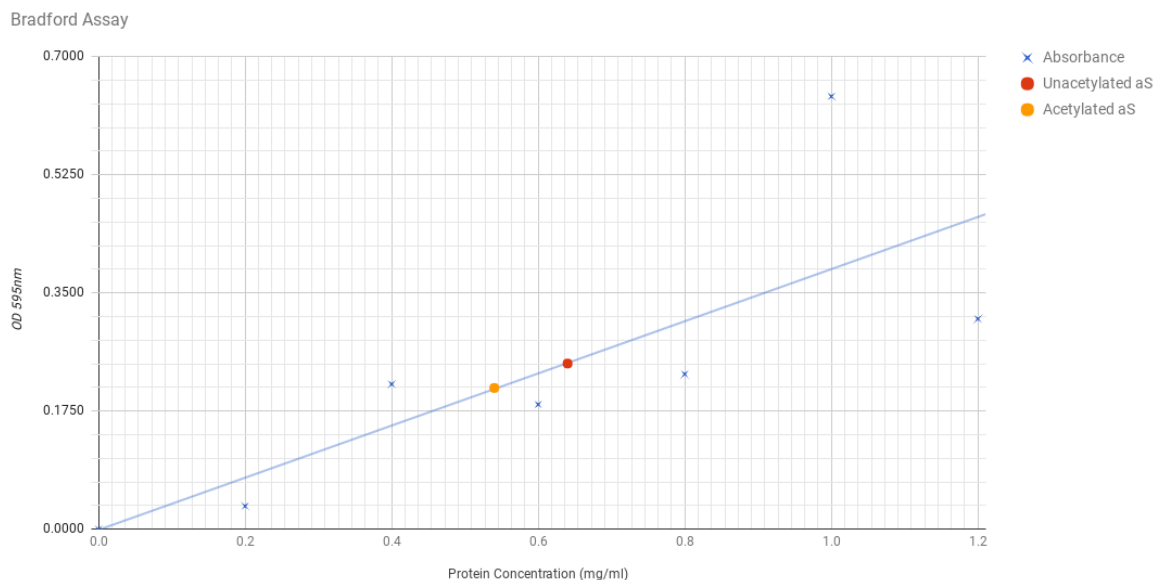
Figure 24: Bradford Assay for protein concentration. The standard curve is shown in blue, whilst un-acetylated αSynuclein (0.64 mg/mL), is shown in red and acetylated αSynuclein (0.54 mg/mL) is shown in orange.

	OD 595	Protein concentration (mg/ml)
Acetylated αS	0.2093	0.54
Un-acetylated αS	0.2455	0.64

**Table 2: αSynuclein protein concentrations** determined using the Bradford assay. Their optical densities were compared to the standard curve in **Figure 24** to obtain their concentration.

We then made up three concentrations of each protein; ⅓µM, 1µM and 3µM and used these in the stopped flow experiments, monitoring light scattering changes at 545nm and fluorescence changes at 436nm.

We began with the analysis of acetylated αSynuclein and DSPG; the concentration of which was maintained at 1mM. At a protein concentration of 1µM, two distinct phases are observed (Figure 25). A rapid initial phase, shown by a rapid decline in amplitude (A1) of -2.56301 and high initial rate (R1) of 19.21794 followed by a slower secondary phase, shown by a much more gradual decrease in amplitude (A2) of -1.79428 and the secondary rate (R2) of 1.88927.

At 3 µM (Figure 26), only one phase is detected. The amplitude of this phase (A) which was -0.67018, is far lower than the amplitude of the initial phase when tested at 1µM, but faster than the secondary phase. This could be due to the initial phase decelerating or the slow phase had accelerating. At 3µM, the initial rate appears to have decreased significantly (R1), and as there is little or no secondary phase, there is no rate for the secondary phase.

Light scattering data was variable making it difficult to monitor, however a similar pattern was seen when the measurement graphs were overlaid over one another (Figure 27). The light scattering at ⅓ µM would increase rapidly followed by a gradual decrease and then would stay at the same level, whereas at 1 µM, there would be an initial increase and the second phase of this data would vary; increasing in some measurements or decreasing in other measurements. The conclusion we reached from this were that concentration of the acetylated αS did make a difference to the fluorescence, indicating a some kind of binding event, and concentration appeared to alter this interaction, particularly the secondary event. Due to the variability of the light scattering data, further analysis is required to make any conclusions from the data collected. Light scattering data using the acetylated protein with the vesicles over the same time period as the un-acetylated protein would also need to be collected.
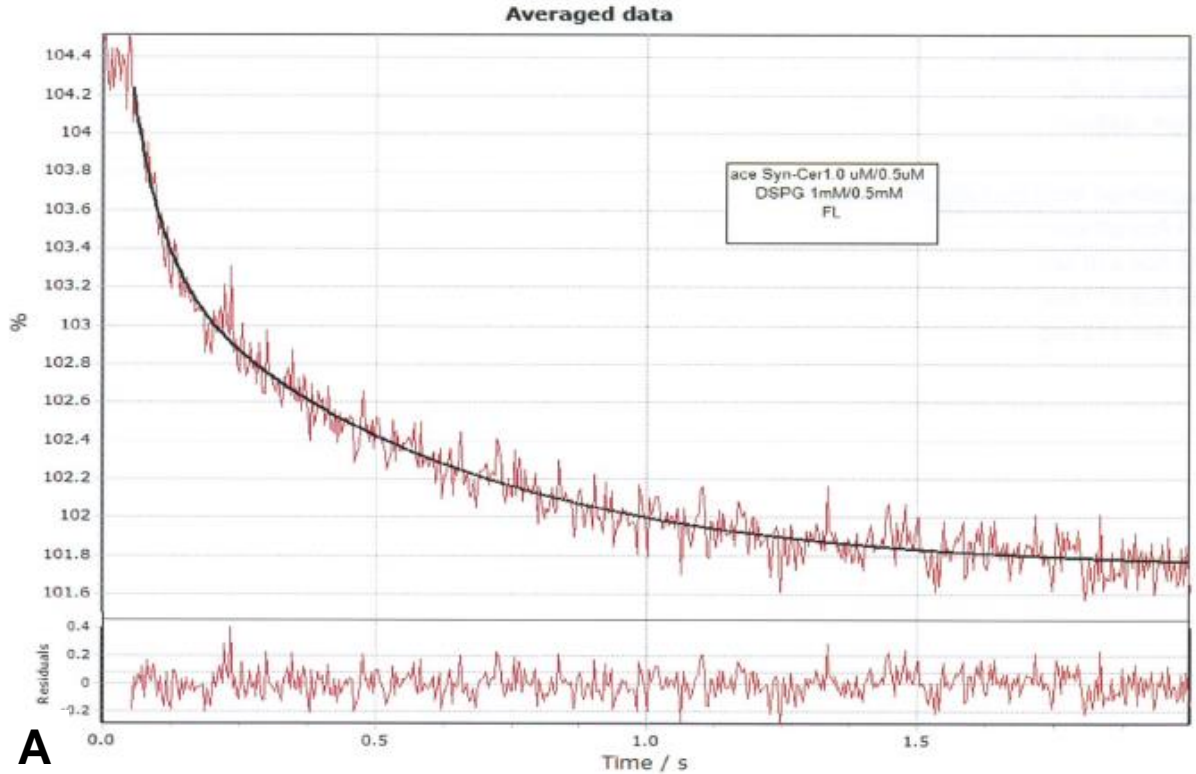
Figure 25: (A) Stopped Flow Fluorescence graph showing the interaction between acetylated αSynuclein at 1 μM and DSPG vesicles at 1mM. Two phases clearly observed; a rapid initial phase and a slower secondary phase. **(B) Corresponding Fit parameter values.** A1 = Amplitude of initial phase, A2= Amplitude of secondary phase, R1 = Rate of initial phase and R2 = Rate of secondary phase.

Averaged data

ace Syn-Cer 3 uM/1.5uM
DSPG 1mM/0.5mM
fl

A
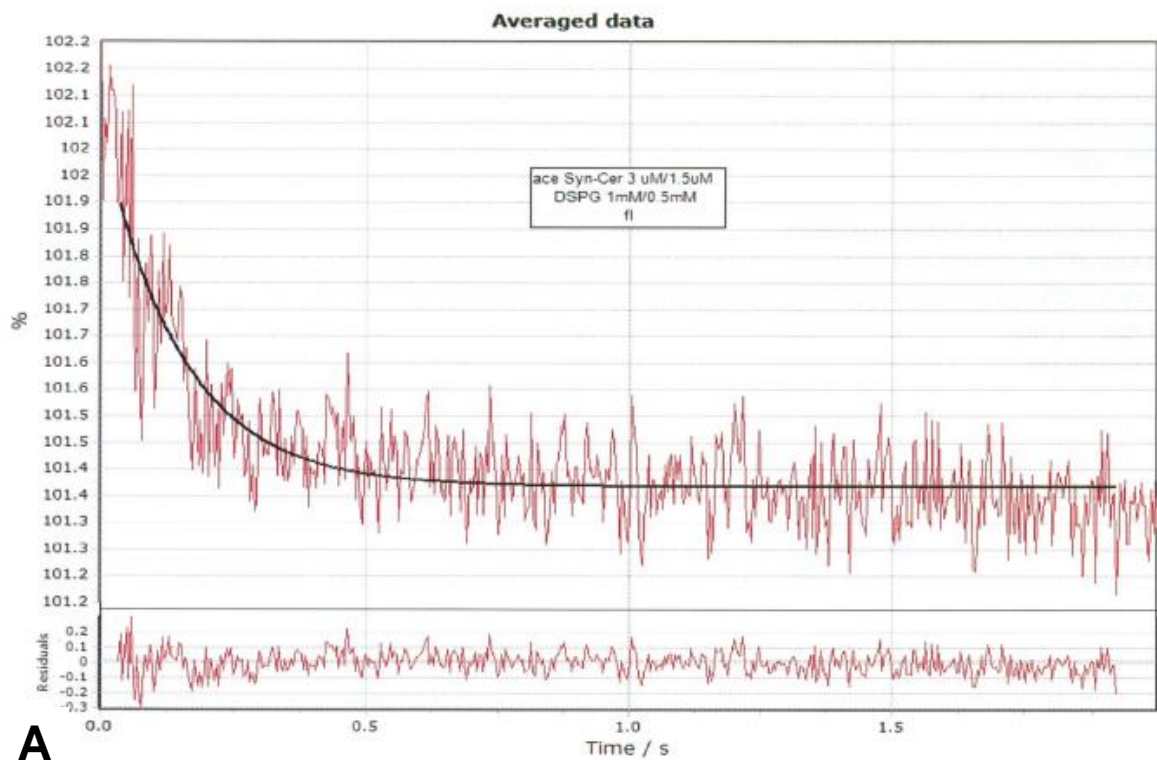
Fit Parameter Name	A	R
Value	-0.67018	6.64585

B

Figure 26: (A) Stopped flow fluorescence graphs showing the interaction between DSPG vesicles at 1mM and acetylated αSynuclein at 3μM. Average of 4 datasets is shown. Only one phase recorded, and a much lower amplitude for the slower phase when compared to the data at 1μM. **(B) Corresponding Fit Parameter values:** A = Amplitude, R1 = Rate
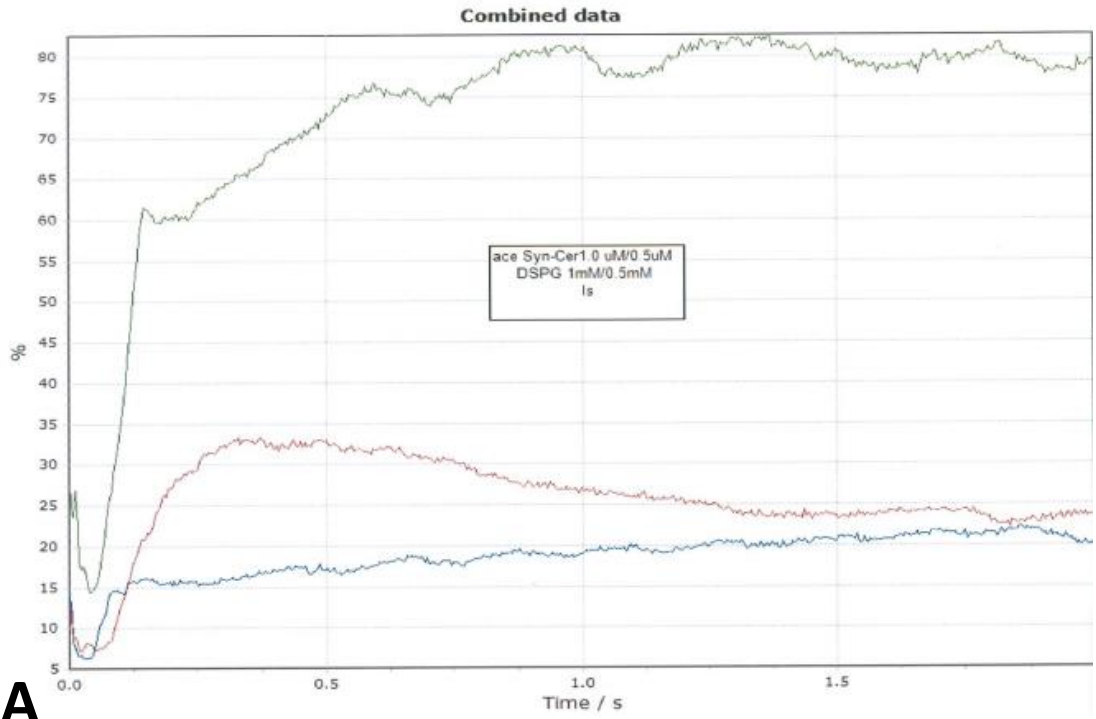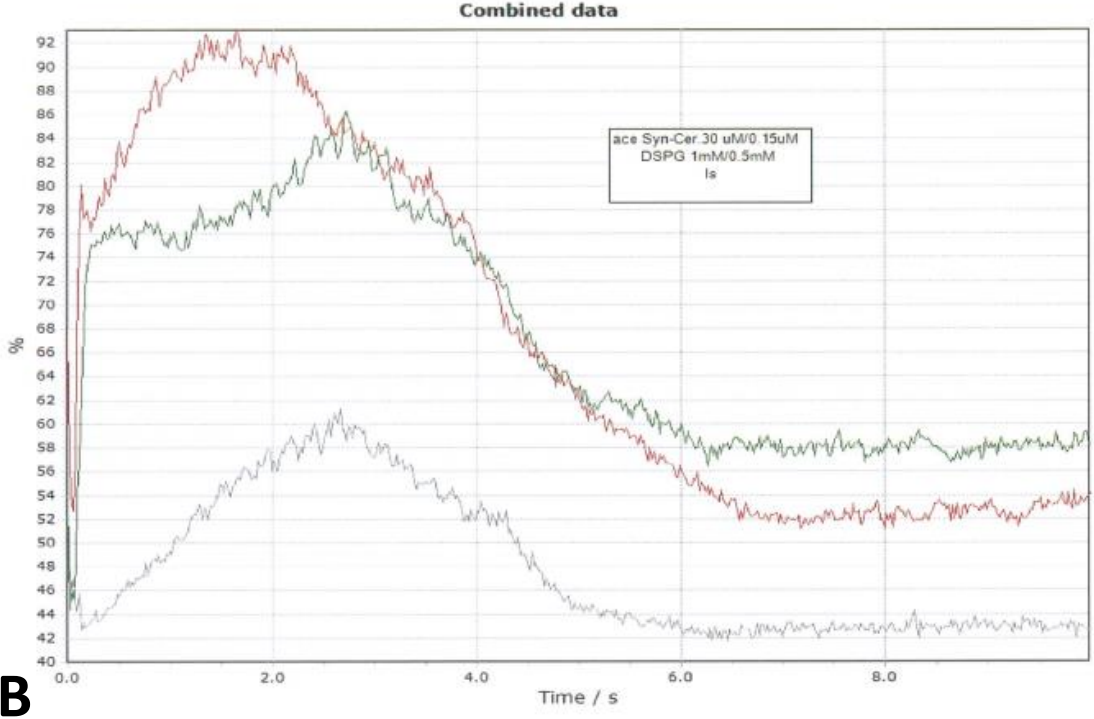
Figure 27: Stopped Flow Light Scattering graphs. *(A)* Acetylated αSynuclein at 1μM interacting with DSPG vesicles at 1mM. Light scattering would increase initially, however in the second phase, this would vary, increasing gradually in some measurements (green and blue lines) or decreasing gradually in other measurements (red line) *(B)* acetylated αSynuclein at ⅓ μM interacting with DSPG vesicles at 1mM over a longer time period (10 seconds) The light scattering Increases initially then gradually decreases, suggesting two phases.

We then began analysis of the un-acetylated αSynuclein with DSPG vesicles (Figures 28 - 30).

The fluorescence for all three concentrations had revealed two phases. Similar to the acetylated protein, a rapid initial phase was observed (A1 and R1) and a more gradual secondary phase was observe (A2 and R2). At ⅓ µM, the amplitude of the initial phase (describing change in fluorescence) was -2.69962, this decreased at 1µM which was -2.34839 but increased at 3µM to -2.75245. The rate, however, of the initial phase (R1) for ⅓ µM was 19.73524, which increased to 22.52082 at 1µM and then increased to 28.17782 at 3µM. This suggests that the initial event, which could possibly be binding, speeds up with increasing concentrations of un-acetylated αSynuclein, however, further experiments would need to be carried out in order to understand the decrease in amplitude from ⅓ µM to 1 µM and then the increase from 1µM to 3µM. The amplitude change of the secondary phase at ⅓ µM (A2) was -1.54217, which then decreased to -0.54706 at 1µM and then decreased again at 3µM to -0.43028. The rate of the secondary phase (R2) at ⅓ µM was 1.18162, which then decreased to 1.16064 at 1µM and further decreased at 3µM to 1. So the rate and amplitude both decreased with increasing concentration, suggesting that the second event slows down with increasing concentration and there is a lower change in fluorescence with increasing concentration. Potentially, this could suggest that the increase in concentration negatively affects the secondary event.

From this data, a concentration dependent interaction is seen. At all concentrations, two distinct phases are seen.

When carrying out light scattering experiments using αSynuclein at both 1µM and 3µM in the absence of vesicles (Figure 31), both traces showed too much noise to make conclusive statements, so light scattering experiments were not carried out. With more time, an investigation into the possible reasons for this would need to be carried out in order to carry out the light scattering experiments.

A
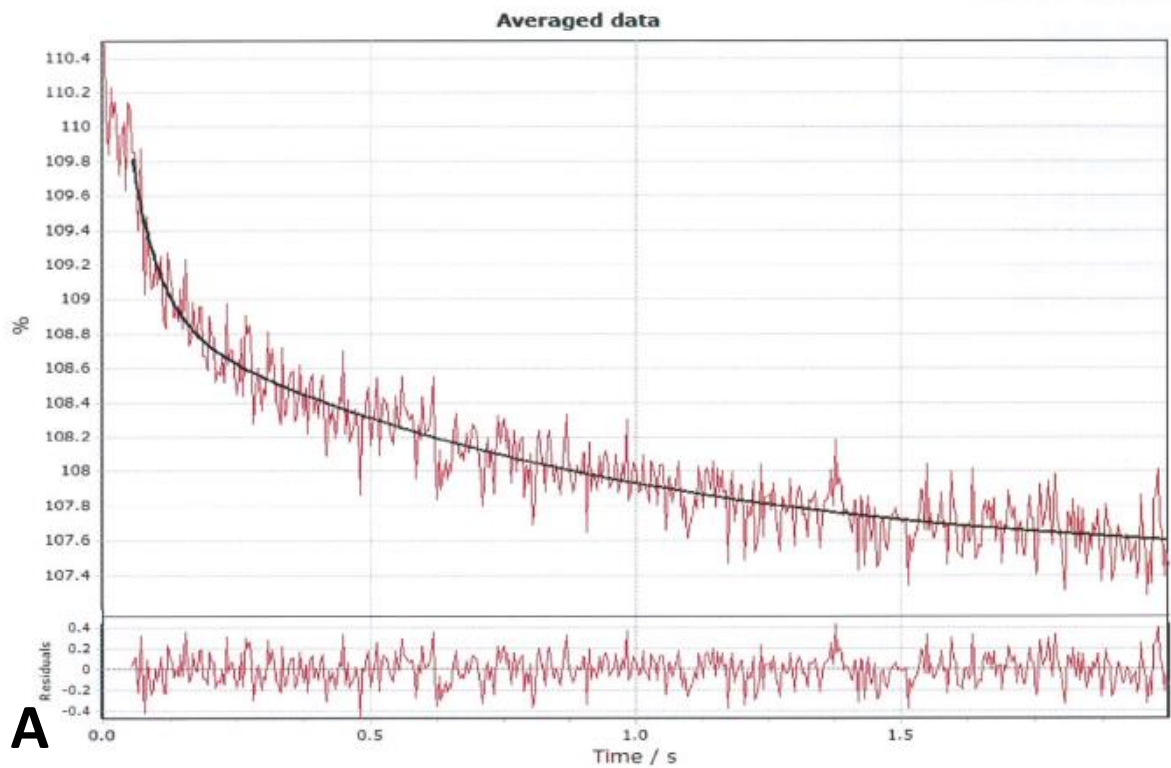
Fit Parameter Name	A1	A2	R1	R2
Value	-2.69962	-1.54217	19.73524	1.18162

B

Figure 28. *(A)* **Averaged fluorescence graphs** showing the interaction between un-acetylated αSynuclein at ⅓ µM and DSPG vesicles at 1mM. *(B)* **Corresponding fit parameter values.** A1 = Amplitude of the initial phase, A2 = amplitude of the secondary phase, R1 = Rate of the initial phase and R2 = Rate of the secondary phase. Two distinct phases, suggesting two distinct events occurring.
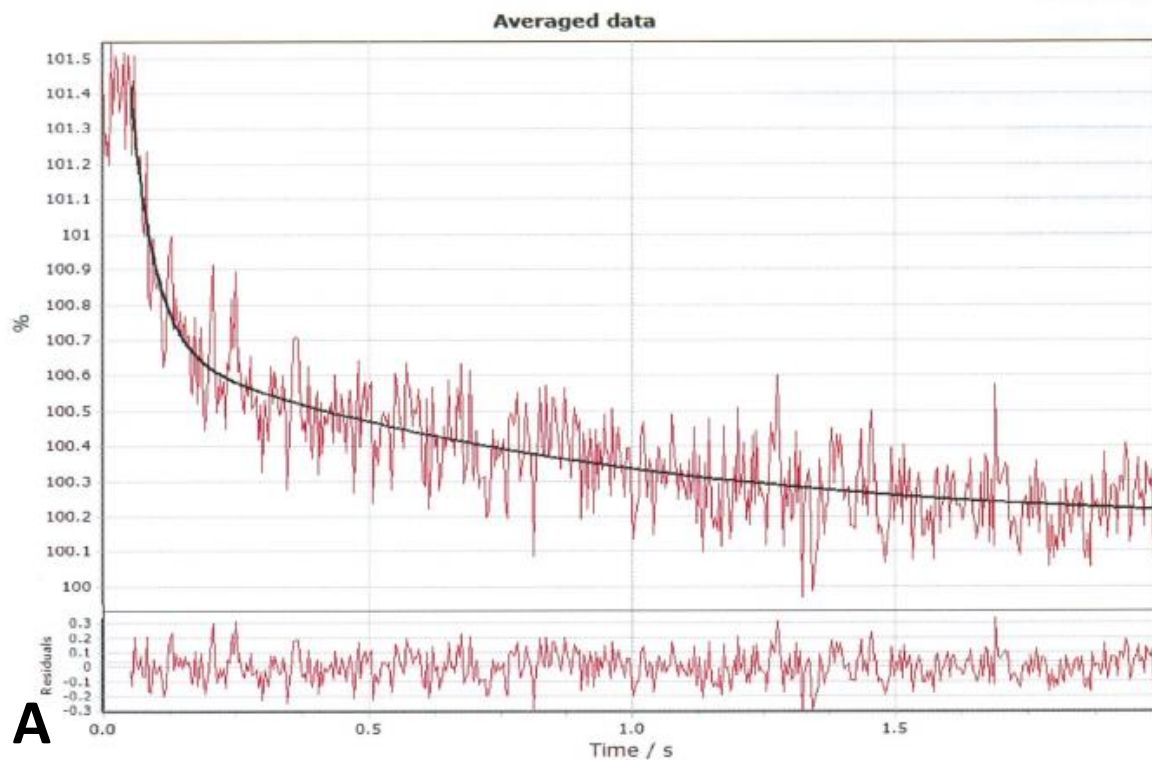
Figure 29: *(A)* **Stopped flow fluorescence graphs** showing the interaction between un-acetylated αSynuclein at 1μM and DSPG vesicles at 1mM. Two distinct phases observed, however a faster initial rate and a slower rate for the secondary phase when compared to the lower concentration. *(B)* **The corresponding fit Parameter values.** A1 = Amplitude of the initial phase, A2 = amplitude of the secondary phase, R1 = Rate of the initial phase and R2 = Rate of the secondary phase. Two distinct phases, suggesting two distinct events occurring.
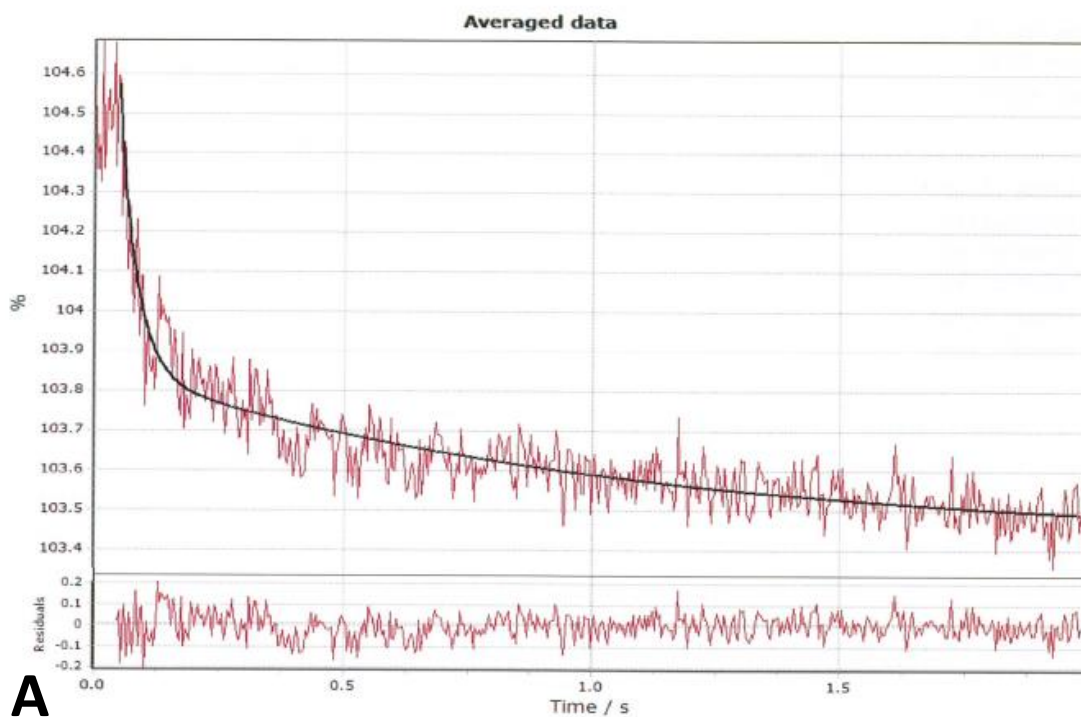
Fit Parameter Name	A1	A2	R1	R2
Value	-2.75245	-0.43028	28.17782	1

Figure 30. *(A)* **Stopped flow Fluorescence graphs (Average of multiple traces)** showing the interaction of un-acetylated αSynuclein at 3µM. A much faster initial rate (A1 and R1) and slower secondary phase (A2 and R3) observed when compared to the two lower concentrations. *(B)* **Corresponding fit parameter values.** A1 = Amplitude of the initial phase, A2 = amplitude of the secondary phase, R1 = Rate of the initial phase and R2 = Rate of the secondary phase.
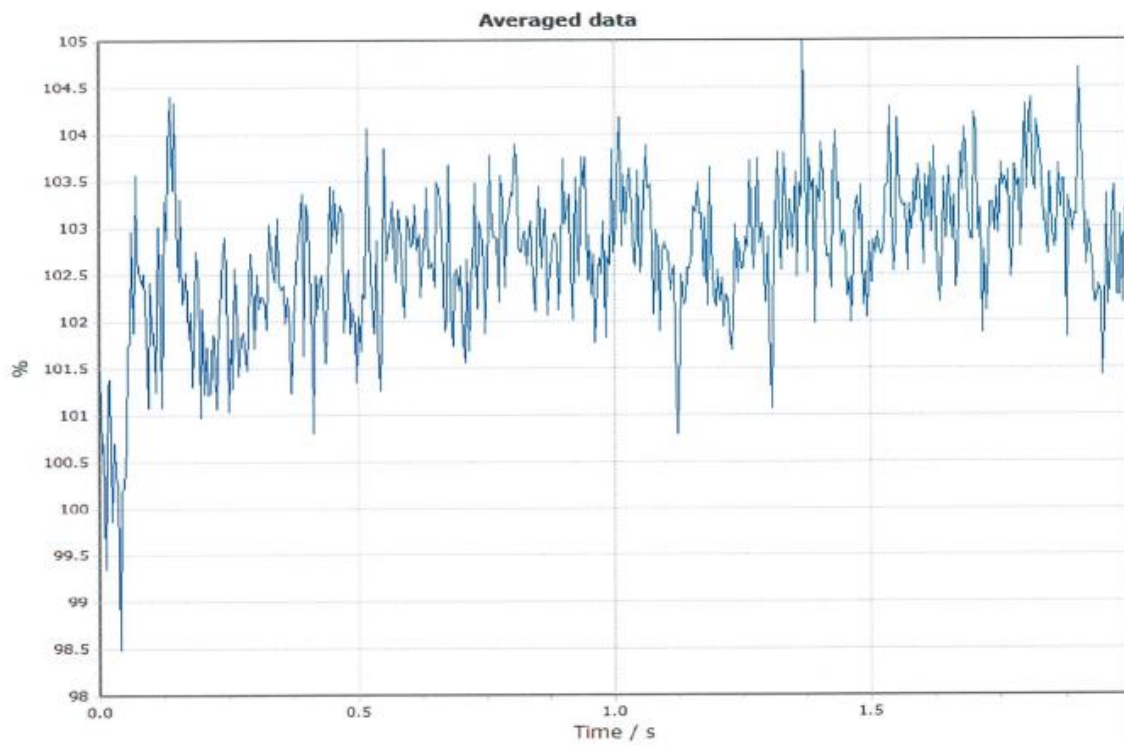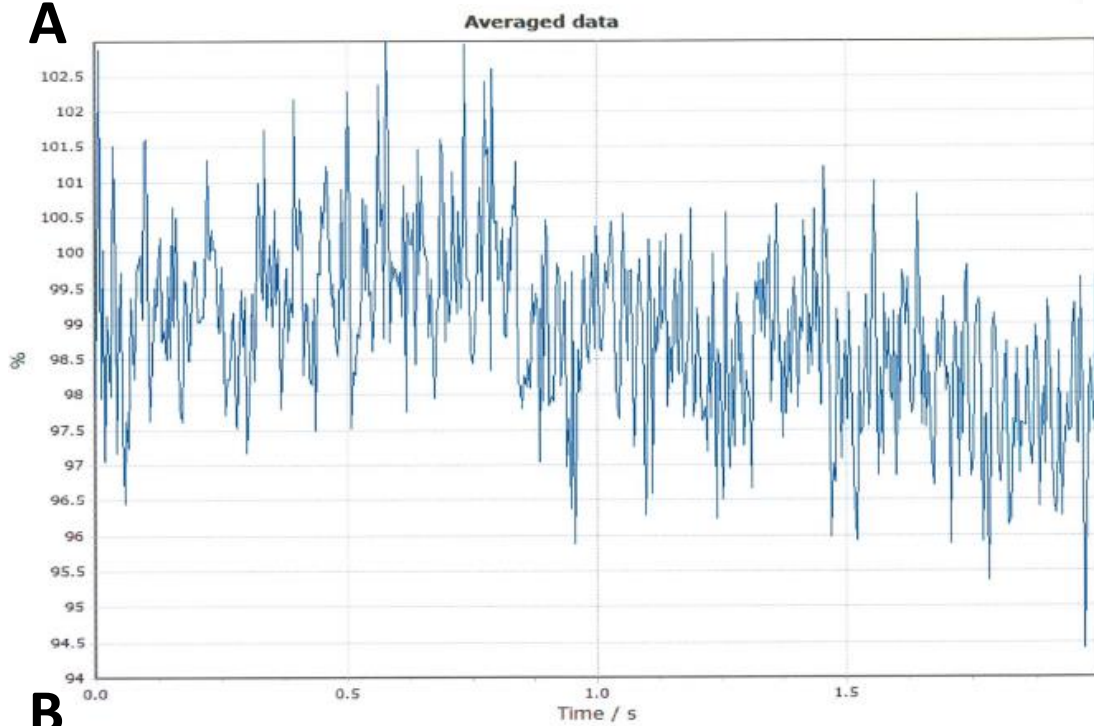
Figure 31: *(A)* **Stopped Flow light scattering graph** for un-acetylated αSynuclein at 3µM in the absence of vesicles *(B)* **Stopped flow light scattering graph** for un-acetylated αSynuclein at 1µM run in the absence of vesicles. Traces showed too much noise to make any conclusive statements from.

Chapter 4

Discussion

4.1 – Hum 1 TH1 Expression and Purification

Myosin 1 subgroups have been shown to vary in function [20, 56], and the presence of the TH1 domain may have a part to play in this, as it has been shown to interact with phospholipids [57]. Understanding the TH1 domain and the difference post translational modifications make to its interactions is important in understanding diseases and also in understanding other similar proteins. From our data we can see that the localization of TH1 and the phosphorylated TH1 were different. Although we successfully cloned, expressed and purified the TH1 domain and the phospho-mutant, we were only able to see the basic interactions that the TH1 domain has with phospholipids. This will provide a basis for future experiments, however future steps in this project would be to use the neon green TH1 in stopped flow and DLS experiments with different phospholipids and compare this with the Neon green phosphomutant and time lapse imaging of the vesicles at a higher magnification. The TH1 domain also has other post translational modifications, so we could look into how they impact Myosin interactions and localization.

4.2 – Hum 1 TH1 Microscopy

As we were unable to clearly visualize vesicles using the SRB imaging technique [55], microscopy experiments with the TH1 domain and different lipid vesicles were not carried out. Further improvement of the microscopy technique would allow us to determine the interaction between the TH1 domain with different phospholipids and the effect of phosphorylation, as well as with other post translational modifications. The microscopy images revealed a difference in the localization in the phosphorylated and wild type TH1, which could be due to the phosphate group increasing solubility in solutions by changing the overall charge of the molecule. Furthermore, the creation of the neon green TH1 would allow us to better visualize the protein. Improvement of this technique would allow us not only to understand the TH1 domain, but other lipid binding proteins whose functions are still unknown, which would benefit the scientific community greatly, as it would allow us to clearly visualize protein-lipid activity.

4.3 – Hum 1 TH1 Vesicle Studies

As shown within this thesis, the sedimentation assays were unsuccessful in determining the interactions the TH1 domain has with various phospholipids. This could be due to the purification method keeping the protein denatured, so it may not have been able to interact with the phospholipids. Optimizing protein expression and purification so that we have natively purified protein could allow us to carry out these experiments. We may also be able to test the TH1 domain against PIP strips, which are nitrocellulose membranes with different phospholipids attached to the surface. However the as DLS studies and co-flotation assays better mimic physiological conditions [58], these techniques would be preferred as they could give us more accurate results [59]. The FM4-64 analysis was unclear, as visual determination of the

presence of the dye was difficult. This could be due to the small amount of the dye being present within the sample, which could have been too dilute to visualize by eye. To overcome this, a full fluorescence scan could be carried out so as to determine the presence of even the smallest amount of dye. However, the Neon green TH1 will allow us to produce more quantifiable data with other simpler techniques, will allow us to track the interactions and possibly visualize them, so we would not take the FM464 analysis method forward for future experiments.

4.4 - Alpha Synuclein

Our data revealed a significant difference in the interactions that the acetylated and un-acetylated αSynuclein had. The DLS studies appeared to suggest that the acetylated αSynuclein would either not interact with the phospholipids (in particular POPC) or in the case of DSPG appeared to mainly aggregate vesicles. However when compared to the stopped flow data, the protein would bind to the vesicles and there would be another event occurring after this. A possible explanation could be that acetylated αSynuclein does interact with DSPG, however no change to the shape or size of the vesicles happens. If the protein is causing vesicle aggregation, then this could explain the changes we see with DLS experiments, and the two phases seen when stopped flow was carried out. Carrying out further experiments, in particular microscopy, once optimized, could allow us to determine whether this is the case. However, this could push research forward; if acetylation of αSynuclein causes aggregation, this could explain the Lewy bodies seen in PD and could play a part in the pathogenesis of PD.

Our experiments with un-acetylated αSynuclein may help us to understand the physiological function of αSynuclein. Our DLS studies suggested that the protein was fusing DSPG vesicles together, but not others. Our hypothesis was further solidified when the DLS studies were compared to the stopped flow data. This was because two distinct phases were observed with stopped flow, which could be the initial binding followed by vesicle fusion. As mentioned previously, further development of the microscopy technique would allow us to visualize the fusion and would push research in this area forward, as the physiological function of αSynuclein is still uncertain. And as this finding is similar to previous work carried out by other members of the lab, we may be able to determine the function of αSynuclein which would make a way for new treatments or even prevention of Parkinson's disease.

Further work with αSynuclein would be to determine the reasons for varied light scattering data, microscopy imaging with lipid vesicles to determine their interactions, in particular DSPG vesicles. We could also collect data for the both proteins at gradual increases in concentration, and use fluorescent vesicles to monitor how this compares to the data retrieved for non-fluorescent vesicles. A breakthrough in this area, as mentioned above, would allow us to understand Parkinson's pathogenesis and potentially cure or treat it.

4.5 – Conclusion

Our aim in this study was to increase an understanding into how various membrane binding proteins may interact in physiological conditions, using lipid vesicles as models for this. We were able to add knowledge into these areas, in particular with αSynuclein, whose function is still uncertain. Although we would need to carry out more experiments to confirm this, we found that αSynuclein, when un-acetylated, bound more strongly to DSPG vesicles, and may have caused them to fuse (seen by our stopped flow data and DLS data). Understanding how it is doing this and why may give us insight into its function. We were not able to make any definitive conclusions with the TH1 domain, and would need to express and purify this natively before we can do so.

Further work using lipid vesicles will also allow us to predict at a very basic level, which phospholipids and therefore membranes that these proteins can interact with and also understand mutations or imbalances that lead to their inability to function properly.

Understanding membrane binding proteins, their functions and regulation allows us to gain a deeper understanding into how the human body works, and also gives us an understanding of diseases. This leads to more effective cures or treatments, preventative strategies for and potentially reversal of harmful diseases. Although we encountered various obstacles during this project, we were able to learn more about these proteins and as more research is carried out in these areas, this knowledge may have many applications in the future.

References

1. Cooper G.M, (2000). The Cell: A Molecular Approach. Cell Membranes. 2nd edition. [WWW Document]. URL: https://www.ncbi.nlm.nih.gov/books/NBK9928/

2. Lumen, (2013). Boundless Biology. Lipids. [WWW Document]. URL: https://courses.lumenlearning.com/boundless-biology/chapter/lipids/

3. Kelly. K., Jacobs. R, (2017). Phospholipid Biosynthesis. AOCS Lipid Library [Online] URL: http://lipidlibrary.aocs.org/Biochemistry/content.cfm?ItemNumber=39191.

4. Berg J.M., Tymoczko J.L., Stryer L, (2000). There Are Three Common Types of Membrane Lipids. [WWW Document]. URL: https://www.ncbi.nlm.nih.gov/books/NBK22361/

5. Nave C.R, (N.D.). Hyperphysics: Glycerol. [WWW Document]. URL: http://hyperphysics.phy-astr.gsu.edu/hbase/Organic/glycerol.html.

6. Bailey. R, (2017). Phospholipids. *Thought Co.* [WWW Document]. URL: https://www.thoughtco.com/phospholipids-373561

7. Alberts. B, Johnson. A, Lewis. J, et al. (2002). Molecular Biology of the Cell: Protein Function. [WWW Document]. URL: https://www.ncbi.nlm.nih.gov/books/NBK26911/

8. SparkNotes Editors, (N.D.). Cell Membranes. [WWW Document]. URL: http://www.sparknotes.com/biology/cellstructure/cellmembranes/section2.rhtml

9. Lodish. H., Berk. A., Zipursky. S.L, et al. (2000). Molecular cell biology: Membrane proteins. [WWW Document]. URL: https://www.ncbi.nlm.nih.gov/books/NBK21570/

10. Kapellos. G.E. Alexiou. T.S. (2013). Modeling momentum and mass transport in cellular biological media: From the molecular to the tissue scale. Transport in Biological Media.

11. Reitsma. S, Slaaf. D.W, Vink. H, Van Zandvoort. M.A.M.J, & oude Egbrink M.G. A. (2007). The endothelial Glycocalyx: composition, functions, and visualization. *Pflugers Archive* 454(3): 345–359.

12. Alberts. B, Johnson. A, Lewis. J, et al. (2002). Molecular Biology of the Cell: Protein Function. [WWW Document]. URL: https://www.ncbi.nlm.nih.gov/books/NBK26911/

13. Drazic. A, Myklebust. L.M, Ree. R, Arnesen. T (2016). The world of protein acetylation. *Biochimica et Biophysica Acta (BBA) – Proteins and Proteomics.* 1864(10): 1372 – 1401.

14. Mechanobio (N.D.). What are motor proteins: Myosin ATPases. [WWW Document]. URL: https://www.mechanobio.info/topics/cytoskeleton-dynamics/motor-activity/

15. Mechanobio (N.D.). What is Myosin: An introduction to the Myosin Superfamily of Proteins. [WWW Document]. URL: https://www.mechanobio.info/cytoskeleton-dynamics/what-are-motor-proteins/what-is-myosin/

16. Mermall. V, Post. P.L, Mooseker. M.S. (1998). Unconventional Myosins in Cell Movement, Membrane Traffic, and Signal Transduction. *Science.* 279 (5350): 527-533.

17. Nambiar. R, McConnell. R. E, Tyska. M. J. (2009). Control of cell membrane tension by myosin-I. *Proceedings of the National Academy of Sciences of the United States of America.* 106(29): 11972–11977.

18. Hartman. M.A, Finan. D, Sivaramakrishnan. S, Spudich. J.A. (2011). Principles of Unconventional Myosin Function and Targeting. *Annual review of cell and developmental biology.* 27:133-155.

19. Mechanobio Info. (N.D.). What are the steps involved in the myosin powerstroke. [WWW Document]. URL: https://www.mechanobio.info/cytoskeleton-dynamics/what-are-motor-proteins/what-steps-are-involved-in-the-myosin-powerstroke/

20. Lordish. H, Berk. A, Zipursky. S.L et al. (2000). Myosin: The Actin Motor Protein. *Molecular Cell Biology.* 4 (18): 3

21. Uyeda. T.Q, Abramson. P.D, Spudich. J.A. (1996). The neck region of the myosin motor domain acts as a lever arm to generate movement. *Proceedings of the National Academy of Sciences of the United States of America.* 93(9):4459-4464.

22. Sammons. M.R, James. M.L, Clayton. J.E, Sladewski. T.E, Sirotkin. V, Lord. M. (2011). A calmodulin-related light chain from fission yeast that functions with myosin-I and PI 4-kinase. *Journal of Cell Science.* 124 (14): 2466-77.

23. Greenberg. M.J, Ostap. E.M. (2013). Regulation and control of myosin-I by the motor and light chain-binding domains. *Trends Cell Biology.* 23 (2): 81-9.

24. Anson. M, Geeves. M. A, Kurzawa. S. E, & Manstein. D. J. (1996). Myosin motors with artificial lever arms. *The EMBO Journal* 15(22): 6069–6074.

25. Lu. Z, Shen. M, Cao. Y, Zhang. H.M, Yao. L.L, Li. X. (2012) Calmodulin Bound to the First IQ Motif Is Responsible for Calcium-dependent Regulation of Myosin 5a. *The Journal of Biological Chemistry.* 287 (20)

26. Walsh M.P. (1994). Calmodulin and the regulation of smooth muscle contraction. *Molecular and Cellular Biochemistry.* 135 (1): 21-41.

27. Greenberg. M.J, Ostap. E.M. (2013). Regulation and control of myosin-I by the motor and light chain-binding domains. *Trends Cell Biology.* 23 (2): 81-9

28. Mazerik. J. N, Kraft. L. J, Kenworthy. A. K, & Tyska. M. J. (2014). Motor and Tail Homology 1 (TH1) Domains Antagonistically Control Myosin-1 Dynamics. *Biophysical Journal.* 106 (3): 649–658.

29. Lemmon. M.A. (2007). Pleckstrin Homology (PH) domains and phosphoinositides. *Biochemical Society symposium.* 74: 81-93.

30. Geli. M. I, Lombardi. R, Schmelzl. B, & Riezman. H. (2000). An intact SH3 domain is required for myosin I-induced actin polymerization. *The EMBO Journal.* 19 (16): 4281–4291.

31. Kurochkina. N, Guha. U. (2013). SH3 Domains: Modules of protein-protein interactions. *Biophysical Reviews.* 5(1): 29 – 39

32. Donavan. K. W, Bretscher. A. (2015). Head-to-tail regulation is critical for the in vivo function of myosin V. *Journal of Cell Biology*. 209 (3): 359.

33. Li. X. D, Jung H. S, Wang. Q, Ikebe. E, Craig. R, Ikebe. M. (2008). The globular tail domain puts on the brake to stop the ATPase cycle of myosin Va. *PNAS*. 105 (4): 1140 – 1145.

34. Langford. G.M. (2002). Myosin-V, a versatile motor for short-range vesicle transport. *Traffic*. 3(12):859-65.

35. Lin. T, Greenberg. M. J, Moore. J. R, Ostap. E. M. (2011). A Hearing-Loss Associated Myo1c Mutation (R156W) Decreases the Myosin Duty Ratio and Force Sensitivity. *Biochemistry*. 50 (11): 1831 – 1838

36. DePina. A. S, Langford. G. M. (1999). Vesicle Transport: The role of actin filaments and myosin motors. *Microscopy Research and Technique.* 47(2).

37. Genetics Home Reference. (N.D.). SCNA Gene. National Library of Medicine. [WWW Document]. URL: https://ghr.nlm.nih.gov/gene/SNCA

38. Braak. H, Del. Tredici. K, Rüb. U, de Vos. R.A, Jansen Steur. E.N, Braak. E. (2003). Staging of brain pathology related to sporadic Parkinson's disease. *Neurobiology of Aging*. 24(2):197-211

39. Barbour. R, Kling. K, Anderson. J. P, Banducci. K, Cole T, Diep. L, Fox. M, Goldstein J. M, Soriano F, Seubert P, Chilcote T. J. (2008). Red Blood Cells Are The Major Source of Alpha Synuclein in Blood. *Neurodegenerative Diseases*. 5: 55-59

40. Spillantini. M.G, Schmidt. M.L, Lee. V.M, Trojanowski. J.Q, Jakes. R, Goedert. M. (1997). Alpha-synuclein in Lewy bodies. Nature. 388(6645):839-40.

41. Ulusoy. A, Decressac. M, Kirik. D, Björklund. A. (2010). Chapter 5 - Viral vector-mediated overexpression of α-synuclein as a progressive model of Parkinson's disease. *Progress in Brain Research*. 184: 89 – 111.

42. Vamvaca. K, Volles. M.J, Lansbury. P.T. (2010). The First N-terminal Amino Acids of α-Synuclein Are Essential for α-Helical Structure Formation In Vitro and Membrane Binding in Yeast. *Journal of Molecular Biology*. 389 (2): 413-424.

43. Iyer. A, Roeters. S.J, Schilderink. N, Hommersom. B, Heeren. R.M.A, Woutersen. S, Claessens. M.M.A.E, Subramaniam. V. (2016). The Impact of N-terminal Acetylation of Alpha Synuclein on Phospholipid Membrane Binding and Fibril Structure. *Journal of Biological Chemistry.*

44. Xu. L, Pu. J. (2016). Alpha-Synuclein in Parkinson's Disease: From Pathogenetic Dysfunction to Potential Clinical Application. *Parkinson's disease*. 1720621.

45. Nemani. V.M, Lu. W, Berge. V, Nakamura. K, Onoa. B, Lee. M.K, Chaudhry F.A, Nicoll R.A, Edwards. R.H. (2010). Increased expression of Alpha Synuclein reduces neurotransmitter release by inhibiting synaptic vesicle reclustering after endocytosis. *Neuron*. 65(1): 66-79.

46. Lee. D, Lee. S.Y, Lee. E.N, Chang. C.S, Paik. S.R. (2004). α-Synuclein exhibits competitive interaction between calmodulin and synthetic membranes. *Journal of Neurochemistry. 82* (5).

47. Mohite. G.M, Kumar. R, Panigrahi. R, Navalkar. A, Singh. N, Datta. D, Mehra. S, Ray. S, Gadhe L.G, Das. S, Singh. N, Chatterjee. D, Kumar. A, Maji. S.K. (2018). Comparison of Kinetics, Toxicity, Oligomer Formation, and Membrane Binding Capacity of α-Synuclein Familial Mutations at the A53 Site, Including the Newly Discovered A53V Mutation. *Biochemistry*.

48. Pace. M. C, Xu. G, Fromholt. S, Howard. J, Giasson. B. I, Lewis. J, Borchelt. D. R. (2018). Differential induction of mutant SOD1 misfolding and aggregation by tau and α-synuclein pathology. *Molecular Neurodegeneration*. 13: 23

49. Dobson. C.M. (1999). Protein misfolding, evolution and disease. *Cell Press*. 24 (9): 329 – 332.

50. Sherman. Y.M, Goldberg. A.L. (2001). Cellular Defenses against Unfolded Proteins A Cell Biologist thinks about Neurodegenerative Diseases. *Neuron*. 29: 15-32.

51. Sezonov. G, Joseleau-Petit. D, & D'Ari. R. (2007). Escherichia coli Physiology in Luria-Bertani Broth. Journal of Bacteriology. 189 (23): 8746–8749

52. Qiagen. (2015). QIAprep® Miniprep Handbook for purification of molecular grade DNA. Fourth edition. [WWW Document]. URL: https://www.qiagen.com/us/resources/resourcedetail?id=22df6325-9579-4aa0-819c-788f73d81a09&lang=en

53. Zhao. H, Lappalainen. P. (2012). A simple guide to biochemical approaches for analysing protein-lipid interactions. *Molecular biology of the cell*. 23(15): 2821-3024.

54. Tronchere. H, Boal. F. (2017). Liposome Flotation Assays for phosphoinositide-protein interaction. *Bio-protocol*. 7(5).

55. Lira. R.B, Steinkühler. J, Knorr R.L, Dimova. R, Riske K.A. (2016). Posing for a picture: vesicle immobilization in agarose gel. *Scientific Reports*. 25254.

56. Kittelberger. N, Breunig. M, Martin. R, Knölker. H.J, Miklavc. P. (2016). The Role of Myosin 1c and Myosin 1b in surfactant exocytosis. *Journal of Cell Science*. 129 (8): 1685 – 1696.

57. Feeser. E.A, Ignacio. C.M.G, Krendel. M, Ostap. E.M. (2010). Myo1e binds anionic phospholipids with high affinity. *Biochemistry.* 49(43): 9353 – 9360.

58. Piascik. M, Zegarlinska. J, Sikorski. A.F, Czogalla. A. (2017). Optimisation of flotation assay conditions for syndapin binding to phosphatidic acid containing liposomes. *Folia Biologica et Oecologica*. 13:9-17.

59. Stetefeld. J, McKenna. S.A, Patel. T.R. (2016). Dynamic Light Scattering: a practical guide and applications in biomedical sciences. *Biophysical Reviews*. 8(4): 409-427.